DOI 10.2478/ama-2023-0068 acta mechanica et automatica, vol.17 no.4 (2023)

EXACT ANALYSIS OF FRACTIONALISED JEFFREY FLUID IN A CHANNEL WITH CAPUTO AND CAPUTO FABRIZIO TIME DERIVATIVE: A COMPARATIVE STUDY

Maryam ASGIR*, Muhammad Bilal RIAZ,***, Ayesha ISLAM*****

*Department of Mathematics, Riphah International University, Lahore, 54000, Pakistan
**Faculty of Applied Physics and Mathematics, Gdansk University of Technology, 80-233 Gdansk, Poland
**Department of Computer Science and Mathematics, Lebanese American University, Byblos, Lebanon
***Department of Mathematics, University of Management and Technology, 54770 Lahore, Pakistan
**Department of Physics, University of Management and Technology, Lahore, 54770, Pakistan

maryam.asghar90@gmail.com, muhammad.riaz@pg.edu.pl, ayesha.islam@umt.edu.pk

received 22 November 2022, revised 17 March 2023, accepted 16 April 2023

Abstract: The non-integer order derivatives, Caputo (C) and Caputo Fabrizio (CF), were employed to analyse the natural convective flow of magnetohydrodynamic (MHD) Jeffrey fluid. The aim is to generalise the idea of Jeffrey's fluid flow. The fluid flow is elaborated between two vertical parallel plates. One plate is kept fixed while the other is moving with the velocity $U_0f(t)$, which induces the motion in the fluid. The fluid flow problem is modelled in terms of the partial differential equation along with generalised physical conditions. The appropriate parameters are introduced to the dimensionless system of equations. To obtain the solutions, the Laplace transform (LT) is operated on the fractional system of equations, and the results are presented in series form. The pertinent parameter's influence on the fluid flow is brought under consideration to reveal interesting results. In comparison, we noticed that the C approach shows better results than CF, and graphs are drawn to show the results. The results for ordinary Jeffrey fluid, second-grade and viscous fluid are obtained in a limiting sense.

Keywords: Jeffrey fluid, porous medium, natural convection, magnetohydrodynamic, Laplace transform, Caputo derivative, Caputo Fabrizio derivative

1. INTRODUCTION

The Navier–Stokes equation cannot characterise the mechanical features of non-Newtonian fluids owing to their complex nature. So, the rheological behaviour of non-Newtonian fluids cannot be described enough with a single constitutive equation. Non-Newtonian fluids with their rheological behaviour makes them valuable for many industrial and technological applications, for instance, in the petroleum, biological, plastic manufacturing, chemical, textile and cosmetic industries. There are several models accorded to describe the resourceful nature of non-Newtonian fluids [1,2]. In addition, Jeffrey fluid is obtained to be the simplest generalisation of the Newtonian fluid. This fluid model is apt for narrating the characteristics of relaxation and retardation times. From the model of Jeffrey fluid, the second-grade and viscous fluid models can be deduced by disregarding the impacts of their generalised parameters. Being mindful of its properties and abilities, the wide application of Jeffrey fluid is noticed in biological science such as in plasma, handling of biological fluid and blood, and in mechanics. Hayat et al. [3] highlighted the chain solution of the magnetohydrodynamic (MHD) Jeffrey fluid in a channel. MHD analysis along with the slip condition on Jeffrey fluid was reported by Das et al. [4]. Imtiaz et al. [5] initiated the study of MHD Jeffrey fluid and highlighted the effects of heterogeneous and homogeneous reactions on the fluid flow. The effects of heat generation on MHD Jeffrey fluid in a porous medium were studied by Jena et al. [6].

Similar studies on MHD Jeffrey fluid are recorded in literature [7–14] and the references therein. The versatile and valuable impacts of fractional calculus in the field of electrical engineering, electrochemistry, control theory, electromagnetism, mechanics, image processing, bioengineering, physics, finance, fluid dynamics and many others make it a valuable tool for study. For systems that have long-term memory, fractional derivatives are very important and suitable because they record not only the present but also the past. It has numerous applications in physical science, such as chemistry, ecology, geology and biology. The mechanism of non-Newtonian models has been elaborated successfully with fractional calculus in the past decades due to its simple and elegant description of the complexity of its behaviour. One of the important non-Newtonian fluids is viscoelastic fluids which exhibit the behaviour of elasticity and viscosity. These fluids have broad implications and importance in several areas of engineering, such as industrial engineering, polymerisation, mechanical engineering and the automobile industry. Fractional calculus is very helpful in interpreting the viscoelastic nature of the materials. Taking into account the enormous properties mentioned, many researchers have paid attention to studying it directly or indirectly in the fractional order derivative field. Bagley and Torvik [15] noted the fractional calculus application on the viscoelastic fluids. Jamil and Khan [16] explored the impacts of slip conditions on the fractional Maxwell fluid and explored the closed solution of shear stress and velocity. Kot and Elmaboud [17] conducted an analysis of heat transfer of the flow of pulsatile time-dependent Maxwell fluid by a vertical stenosed artery with body acceleration. They employed the Cattaneo fractional model to modify the energy equation. Riaz et al. [18] analysed the impacts of heat transfer on MHD fractionalised Oldroyd-B fluid. Semi-analytic and numerical solutions are attained for the electroosmotic flow of the fractionalised Oldroyd-B fluid by Alsharif et al. [19]. The flow takes place in a vertical microchannel that is filled with a porous medium. Khan et al. [20] investigate the Casson fluid with the Caputo (C) time derivative. The C and Caputo Fabrizio (CF) comparative analysis of second-grade fluid with Newtonian heating was investigated by Imran et al. [21]. To reveal the interesting facts on the electroosmotic flow of second-grade fluid, an intriguing study was done by Abdellateef et al. [22]. The flow happens through the vertical microchannel. They considered the heat equation and modified it with the Cattaneo heat flux model and revealed interesting results. Alsharif and Elmaboud [23] considered the above-said problem in the vertical annulus. They solved the problem with the finite Hankel transform and Laplace transform. The results show that as the volume concentration rise, the hybrid nanofluid becomes more viscous, and electroosmotic flow is accelerated by free convection force. Saqib et al. [24] studied the natural convective flow of generalised Jeffrey fluid with the CF approach. Shehzad et al. [25] demonstrate the problem of 3D MHD flow of the Jeffrey fluid along with Newtonian heating. Hayat et al. [26] examined the MHD flow of the Jeffrey fluid through a channel and discovered the series solutions. Farman et al. [27] conducted research to investigate the complex action of the COVID-19 Omicron variant with the CF derivative. A numerical scheme is employed for the computational and simulation of the COVID-19 model. Some of the contributions of the fractional calculus on the viscoelastic fluids are highlighted in literature [28–38].

Inspired by the above literature, this article is devoted to studying the heat and mass transfer analysis of the MHD fractional Jeffrey fluid through a channel along with generalised boundary conditions. In the paper layout, Section 2 describes the governing equation with the geometry of the problem. Preliminaries are stated in Section 3. In Section 4, we have converted the integer-order derivative Jeffrey fluid model with the fractional order derivative C and CF model. The Laplace transform (LT) has been employed to attain the analytical solutions. The analytical expression for velocity, temperature, and concentration are evaluated in a series form. Such exact solutions have never been noted in the literature before. Hence this article makes valuable contributions to the existing literature in view of the pancity of exact solutions of Jeffrey fluid with generalised boundary conditions. In Section 5, limiting cases are discussed. The impacts of parameters on the fluid flow, heat and mass distributions, are captured with the assistance of graphs stated in Section 6. The final conclusions are stated in Section 7.

Tab. 1. Nomenclature

Symbol	Quantity
w	Velocity
B_0	Magnetic force
q	LT Parameter
ϑ	Temperature
k	Heat Conduction
ρ	Density
λ	Relaxation time
σ	Electric Conductivity
μ	Viscosity (Dynamic)
υ	Viscosity (Kinematic)
cp	Specific heat
g	Gravitational force
H_a^2	Hartman number
P_r	Prandtl number
G_r	Grashof number(thermal)
K	Porosity
λ_1	Jeffrey fluid parameter
D	Mass diffusivity
G_c	Grashof number(mass)
S_c	Schmidt number

2. MODEL GOVERNING EQUATIONS

The phenomenon of heat and mass transfer of the convective MHD Jeffrey fluid flow is examined. The fluid is submerged in a permeable medium between two upright plates at $\xi^* = 0$ and $\xi^* = d$. At $t^* = 0$, plates and fluid are both static with the ambient temperature ϑ_∞ and concentration ϕ_∞. As $t^* > 0$, the plate at the $\xi^* = 0$ starts to move with velocity $U_0 f(t^*)$, while the other plate is kept fixed. The temperature of the plate descends or ascends to $\vartheta_d + (\vartheta_w - \vartheta_d)g(t^*)$, and concentration $\phi_d + (\phi_w - \phi_d)h(t^*)$, where $f(t^*), g(t^*)$ and $h(t^*)$ are continuous functions and have zero value at $t^* = 0$. Furthermore, a transverse magnetic force is introduced vertically to the fluid flow. By neglecting the impacts of an induced magnetic field, Joule heating, viscous dissipation and assuming that the velocity is a function of ξ^* and t^* only, the governing equation for the fluid flow description using Boussinesq approximation [39, 40] along with concentration equation will take the form

$$\frac{\partial \omega(\zeta^*,t^*)}{\partial t^*} = \frac{\upsilon}{1+\lambda_1}\left(1+\lambda_r \frac{\partial}{\partial t^*}\right)\frac{\partial^2 \omega(\zeta^*,t^*)}{\partial {\zeta^*}^2} - \left(\frac{\nu\phi}{k_1} + \frac{\sigma {B_0}^2}{\rho}\right)\omega(\zeta^*,t^*) + g\beta_\vartheta(\vartheta_w - \vartheta_d) + g\beta_\phi(\phi - \phi_d), \quad (1)$$

$$\rho C_p \frac{\partial \vartheta(\zeta^*,t^*)}{\partial t^*} = k\frac{\partial^2 \vartheta(\zeta^*,t^*)}{\partial {\zeta^*}^2}, \quad (2)$$

$$\frac{\partial \phi(\zeta^*,t^*)}{\partial t^*} = D\frac{\partial^2 \phi(\zeta^*,t^*)}{\partial {\zeta^*}^2}. \quad (3)$$

The system imposed conditions related to the present problem are

$$\omega(\zeta^*,0) = 0, \frac{\partial \omega(\zeta^*,t^*)}{\partial t^*} = 0, \omega(\zeta^*,0) = 0, \phi(\zeta^*,0) = 0, \quad (4)$$

$$\omega(0,t^*) = U_0 f(t^*),\ \omega(d,t^*) = 0, \quad (5)$$

$$\vartheta(0,t^*) = \vartheta_d + g(t^*)(\vartheta_w - \vartheta_d),\ \vartheta(d,t^*) = \vartheta_w, \quad (6)$$

$$\phi(0,t^*) = \phi_d + h(t^*)(\phi_w - \phi_d),\ \phi(d,t^*) = \phi_w. \quad (7)$$

For the process of dimensionalisation, the following constants and parameters are introduced as

$$\omega' = \frac{\omega}{U_0}, \zeta' = \frac{\zeta^*}{d}, \vartheta' = \frac{\vartheta - \vartheta_d}{\vartheta_w - \vartheta_d}, t' = \frac{\nu t^*}{d^2}, P_r = \frac{\mu c_p}{k}, S_c = \frac{\upsilon}{D}, K = \frac{k_1}{\phi d^2}, \lambda = \frac{\lambda_r \upsilon}{d^2},$$

$$H_a^2 = \sqrt{\frac{\sigma}{\mu}} B_0 d, G_r = \frac{g\beta_\vartheta \upsilon(\vartheta_w - \vartheta_d)}{U_0^3}, G_c = \frac{g\beta_\phi \upsilon(\phi_w - \phi_d)}{U_0^3}. \quad (8)$$

After implementing Eq. (8) into Eqs (1)–(7), the governing equations are expressed after dropping the "/"

$$\frac{\partial \omega(\zeta,t)}{\partial x} = \frac{1}{1+\lambda_1}\left(1+\lambda\frac{\partial}{\partial t}\right)\frac{\partial^2 \omega(\zeta,t)}{\partial \xi^2} - \left(\frac{1}{K} + H_a^2\right)\omega(\zeta,t) + G_r\vartheta(\zeta,t) + G_c\phi(\zeta,t), \tag{9}$$

$$P_r\frac{\partial \vartheta(\zeta,t)}{\partial t} = \frac{\partial^2\vartheta(\zeta,t)}{\partial \xi^2}, \tag{10}$$

$$S_c\frac{\partial \phi(\zeta,t)}{\partial t} = \frac{\partial^2\phi(\zeta,t)}{\partial \xi^2}, \tag{11}$$

The imposed conditions in Eqs (4)–(7) for the velocity, temperature and concentration profiles become

$$\omega(\zeta,0) = 0, \frac{\partial\omega(\zeta,0)}{\partial t} = 0, \ \vartheta(\zeta,0) = 0, \phi(\zeta,0) = 0, \tag{12}$$

$$\omega(0,t) = f(t), \omega(1,t) = 0, \vartheta(0,t) = g(t), \vartheta(1,t) = 1, \phi(0,t) = h(t), \phi(1,t), \tag{13}$$

where all the quantities and parameters are stated in the nomenclature section.

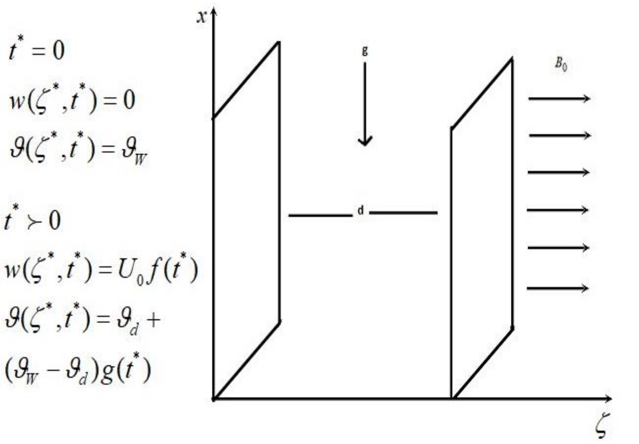

Fig. 1. Geometrical description of the fluid flow phenomenon

3. PRELIMINARIES

The function/non-integer C time derivative is stated as

$${}^{C}D_t^{\eta}h(\sigma,t) = \frac{1}{\Gamma(1-\eta)}\int_0^t (t-\varrho)^{-\eta}R'(\sigma,\varrho)d\varrho, \quad \eta\in(0,1). \tag{14}$$

Implement the LT on the C time derivative

$$L\left({}^{C}D_t^{\eta}R(\sigma,t)\right) = s^nL(R(\sigma,t) - s^{n-1}R(\sigma,0). \tag{15}$$

The non-integer CF time derivative is defined as

$${}^{CF}D_t^{\eta}R(\sigma,t) = \frac{1}{(1-\eta)}\int_0^t e^{\left(\frac{-\eta(t-\varrho)}{1-\eta}\right)}R'(\sigma,\varrho)d\varrho, \quad \eta\in(0,1) \tag{16}$$

Applying the LT on the time fractional CF derivative changes to

$$L\left({}^{CF}D_t^{\eta}R(\sigma,t)\right) = \frac{sL(R(\sigma,t))-R(\sigma,0)}{s(1-\eta)+\eta}. \tag{17}$$

4. FRACTIONAL FORMULATIONS OF GOVERNING EQUATIONS AND SOLUTIONS

4.1. Caputo formulation and solutions

Replace the time derivative with the C fractional derivative into Eqs (9)–(11) as,

$${}^{C}D_t^{\eta}\omega(\zeta,t) = \frac{1}{1+\lambda_1}\left(1+\lambda^{C}D_t^{\eta}\right)\frac{\partial^2\omega(\zeta,t)}{\partial\xi^2} - \left(\frac{1}{K}+H_a^2\right)\omega(\zeta,t) + G_r\vartheta(\zeta,t) + G_c\phi(\zeta,t), \tag{18}$$

$$P_r\,{}^{C}D_t^{\eta}\vartheta(\zeta,t) = \frac{\partial^2\vartheta(\zeta,t)}{\partial\xi^2}, \tag{19}$$

$$S_c\,{}^{C}D_t^{\eta}\phi(\zeta,t) = \frac{\partial^2\phi(\zeta,t)}{\partial\xi^2}, \tag{20}$$

4.1.1 Investigation of exact solution for temperature profile

Implementing LT on Eq. (19), we will obtain with transform boundary conditions

$$\frac{\partial^2\bar{\vartheta}(\zeta,q)}{\partial\xi^2} - P_rq^n\bar{\vartheta}(\zeta,q) = 0, \tag{21}$$

$$\bar{v}(0,q) = G(q), \ \bar{v}(1,q) = \frac{1}{q}. \tag{22}$$

Employing the Laplace transformed boundary conditions stated in Eq. (22), the solution for Eq. (21) will be as obtained in literature [40]

$$\bar{v}(\zeta,q) = qG(q)\left(\frac{sinh((1-\zeta)}{qsinh(\sqrt{P_rq^n})}\right) + \left(\frac{sinh(\zeta\sqrt{P_rq^n})}{qsinh(\sqrt{P_rq^n})}\right) = qG(q)\vartheta_1(\zeta,q) + \vartheta_2(\zeta,q). \tag{23}$$

Here,

$$\vartheta_1(\zeta,q) = \frac{e^{(1-\zeta)\sqrt{P_rq^n}} - e^{-(1-\zeta)\sqrt{P_rq^n}}}{q\left(e^{\sqrt{P_rq^n}} - e^{-\sqrt{P_rq^n}}\right)} = \sum_{n=0}^{\infty}\left(\frac{e^{-(2n-\zeta)\sqrt{P_rq^n}}}{q} - \frac{e^{-(2n+2-\zeta)\sqrt{P_rq^n}}}{q}\right). \tag{24}$$

$$\vartheta_1(\zeta,q) = \sum_{n=0}^{\infty}\left(\sum_{k=0}^{\infty}\frac{(-1)^k(2n+\zeta)^k(P_r)^{k/2}}{k!\Gamma\left(1-\frac{k\eta}{2}\right)}t^{-\frac{k\eta}{2}} - \sum_{k=0}^{\infty}\frac{(-1)^k(2n+2-\zeta)^k(P_r)^{k/2}}{k!\Gamma\left(1-\frac{k\eta}{2}\right)}t^{-\frac{k\eta}{2}}\right). \tag{25}$$

The expression of $\vartheta_2(\zeta, q)$ is in an expanded from defined as below

$$\vartheta_2(\zeta,q) = \frac{e^{\zeta\sqrt{P_rq^n}} - e^{-\zeta\sqrt{P_rq^n}}}{q\left(e^{\sqrt{P_rq^n}} - e^{-\sqrt{P_rq^n}}\right)} = \sum_{n=0}^{\infty}\left(\frac{e^{-(2n+1-\zeta)\sqrt{P_rq^n}}}{q} - \frac{e^{-(2n+1-\zeta)\sqrt{P_rq^n}}}{q}\right). \tag{26}$$

Implement the inverse LT in Eq. (26) as

$$\vartheta_2(\zeta,t) = \sum_{n=0}^{\infty}\left(\sum_{k=0}^{\infty}\frac{(-1)^k(2n+1-\zeta)^k(P_r)^{k/2}}{k!\Gamma\left(1-\frac{k\eta}{2}\right)}t^{-\frac{k\eta}{2}} - \sum_{k=0}^{\infty}\frac{(-1)^k(2n+1+\zeta)^k(P_r)^{k/2}}{k!\Gamma\left(1-\frac{k\eta}{2}\right)}t^{-\frac{k\eta}{2}}\right). \tag{27}$$

DOI 10.2478/ama-2023-0068

Now apply the inverse LT in Eq. (23) as

$$\vartheta(\zeta,t)=\int_0^t g'(t-\tau)\vartheta_1(\zeta,\tau)d\tau+\vartheta_2(\zeta,t), \tag{28}$$

where $\vartheta_1(\zeta,t)$ and $\vartheta_2(\zeta,t)$ are presented in Eqs (25) and (27) respectively.

4.1.2 Investigation of exact solution for concentration profile

Implementing LT on Eq. (20), and bearing the definition of LT of C derivative, we get

$$\frac{\partial^2\phi(\zeta,t)}{\partial\xi^2}=S_c\,q^n\bar{\phi}(\zeta,q)=0, \tag{29}$$

Along with the transformed boundary conditions

$$\bar{\phi}(0,q)=H(q),\ \bar{\phi}(1,q)=\frac{1}{q}. \tag{30}$$

Inserting the prescribed boundary conditions of Eq. (30) while solving Eq. (29), the solution obtained will be

$$\bar{\phi}(\zeta,q)=qH(q)\left(\frac{sinh\left((1-\zeta)\sqrt{S_cq^n}\right)}{qsinh\left(\sqrt{S_cq^n}\right)}\right)+\left(\frac{sinh\left(\zeta\sqrt{S_cq^n}\right)}{qsinh\left(\sqrt{S_cq^n}\right)}\right), \tag{31}$$

To find the solution $\phi_1(\zeta,q)$, we write it in a simplified form as below

$$\phi_1(\zeta,q)=\frac{e^{(1-\zeta)\sqrt{S_cq^n}}-e^{-(1-\zeta)\sqrt{S_cq^n}}}{q\left(e^{\sqrt{S_cq^n}}-e^{-\sqrt{S_cq^n}}\right)}=\sum_{n=0}^{\infty}\left(\frac{e^{-(2n-\zeta)\sqrt{S_cq^n}}}{q}-\frac{e^{-(2n+2-\zeta)\sqrt{S_cq^n}}}{q}\right). \tag{32}$$

Implement the inverse LT in Eq. (32) as

$$\phi_1(\zeta,q)=\sum_{n=0}^{\infty}\left(\sum_{k=0}^{\infty}\frac{(-1)^k(2n+\zeta)^k(S_c)^{k/2}}{k!\Gamma\left(1-\frac{k\eta}{2}\right)}t^{-\frac{k\eta}{2}}-\sum_{k=0}^{\infty}\frac{(-1)^k(2n+2-\zeta)^k(S_c)^{k/2}}{k!\Gamma\left(1-\frac{k\eta}{2}\right)}t^{-\frac{k\eta}{2}}\right). \tag{33}$$

The expression of $\phi_2(\zeta,q)$ in the simplest form is

$$\phi_1(\zeta,q)=\frac{e^{\sqrt{S_cq^n}}-e^{-\zeta\sqrt{S_cq^n}}}{q\left(e^{\sqrt{S_cq^n}}-e^{-\sqrt{S_cq^n}}\right)}=\sum_{n=0}^{\infty}\left(\frac{e^{-(2n+1-\zeta)\sqrt{S_cq^n}}}{q}-\frac{e^{-(2n+1+\zeta)\sqrt{S_cq^n}}}{q}\right). \tag{34}$$

And employing the inverse LT on Eq. (34), the solution will be

$$\phi_2(\zeta,t)=\sum_{n=0}^{\infty}\left(\sum_{k=0}^{\infty}\frac{(-1)^k(2n+1-\zeta)^k(S_c)^{k/2}}{k!\Gamma\left(1-\frac{k\eta}{2}\right)}t^{-\frac{k\eta}{2}}-\sum_{k=0}^{\infty}\frac{(-1)^k(2n+1+\zeta)^k(S_c)^{k/2}}{k!\Gamma\left(1-\frac{k\eta}{2}\right)}t^{-\frac{k\eta}{2}}\right). \tag{35}$$

Now apply the inverse LT on Eq. (31) as

$$\phi(\zeta,t)=\int_0^t h'(t-\tau)\phi_1(\zeta,\tau)d\tau+\phi_2(\zeta,t), \tag{36}$$

where $\phi_1(\zeta,t)$ and $\phi_2(\zeta,t)$ are presented in Eqs (33) and (35), respectively.

4.1.3 Investigation of exact solution for velocity profile

Applying the LT into Eq. (18), we get

$$\left(\frac{1+\lambda q^n}{1+\lambda_1}\right)\frac{\partial^2\bar{\omega}(\zeta,q)}{\partial\xi^2}-\left(q^n+\frac{1}{k}+H_\alpha^2\right)\bar{\omega}(\zeta,q)=-G_r\bar{\vartheta}(\zeta,t)-G_c\bar{\phi}(\zeta,t). \tag{37}$$

After rearranging the above equation, we attain

$$\frac{\partial^2\bar{\omega}(\zeta,q)}{\partial\xi^2}-\Upsilon_1\bar{\omega}(\zeta,q)=\frac{-G_r}{\Upsilon_0}\bar{\vartheta}(\zeta,t)-\frac{-G_c}{\Upsilon_0}\bar{\phi}(\zeta,t), \tag{38}$$

where $\Upsilon_0=\frac{1+\lambda q^n}{1+\lambda_1}$, $\Upsilon_1=q^n+\frac{1}{k}+H_\alpha^2$, $\Upsilon_2=\frac{\Upsilon_1}{\Upsilon_0}$.

The Laplace boundary conditions are

$$\bar{\omega}(0,q)=F(q),\bar{\omega}(1,q)= \tag{39}$$

Introducing Eqs (23) and (31) into Eq. (38), the velocity solution in abridged form is

$$\begin{aligned}\bar{\omega}(\zeta,q)=&\frac{F(q)}{sinh\sqrt{\Upsilon_2}}sinh\left((1-\zeta)\sqrt{\Upsilon_2}\right)+\\&\frac{G_r}{q\Upsilon_0(P_rq^n-\Upsilon_2)sinh\sqrt{\Upsilon_2}}\left(qG(q)\sinh(1-\zeta)\sqrt{\Upsilon_2})-\sinh\left(\zeta\sqrt{\Upsilon_2}\right)\right)-\\&\frac{G_r}{q\Upsilon_0(P_rq^n-\Upsilon_2)sinh\sqrt{P_rq^n}}\left(qG(q)\sinh(1-\zeta)\sqrt{P_rq^n})-\sinh\left(\zeta\sqrt{P_rq^n}\right)\right)+\\&\frac{G_c}{q\Upsilon_0(S_cq^n-\Upsilon_2)sinh\sqrt{\Upsilon_2}}\left(qH(q)\sinh(1-\zeta)\sqrt{\Upsilon_2})-\sinh\left(\zeta\sqrt{\Upsilon_2}\right)\right)-\\&\frac{G_c}{q\Upsilon_0(S_cq^n-\Upsilon_2)sinh\sqrt{S_cq^n}}\left(qH(q)\sinh(1-\zeta)\sqrt{S_cq^n})-\sinh\left(\zeta\sqrt{S_cq^n}\right)\right).\end{aligned} \tag{40}$$

In order to find its inverse Laplace, we write the velocity expression in a suitable form

$$\bar{\omega}(\zeta,q)=\omega_1(\zeta,q)+\omega_2(\zeta,q)-\omega_3(\zeta,q)+\omega_4(\zeta,q)-\omega_5(\zeta,q) \tag{41}$$

$where$

$$\begin{aligned}\omega_1(\zeta,q)&=\frac{F(q)}{sinh\sqrt{\Upsilon_2}}sinh\left((1-\zeta)\sqrt{\Upsilon_2}\right),\\&=F(q)\frac{e^{(1-\zeta)\sqrt{\Upsilon_2}}-e^{-(1-\zeta)\sqrt{\Upsilon_2}}}{e^{\sqrt{\Upsilon_2}}-e^{-\sqrt{\Upsilon_2}}},\\&=F(q)\sum_{n=0}^{\infty}\left(e^{-(2n+\zeta)\sqrt{\Upsilon_2}}-e^{-(2n+2+\zeta)\sqrt{\Upsilon_2}}\right).\end{aligned} \tag{42}$$

Eq. (42) in the simplest form as

$$\omega_1(\zeta,q)=F(q)((P(\zeta,q)-Q(\zeta,q)), \tag{43}$$

where

$$P(\zeta,q)=e^{-(2n+\zeta)\sqrt{\Upsilon_2}}=\sum_{n=0}^{\infty}\sum_{k=0}^{\infty}\frac{(-\Upsilon_3)^k}{k!}\sum_{l=0}^{\infty}\frac{\Gamma\left(\frac{k}{2}+1\right)}{\left(\frac{k}{2}-l+1\right)}\left(\frac{1}{\lambda}\right)^{\frac{k}{2}-l}\left(b-\frac{1}{\lambda}\right)^l\sum_{p=0}^{\infty}(-1)^p\frac{\Gamma(l+p)}{p!\Gamma l}\lambda^pq^{\eta p}, \tag{44}$$

where $\Upsilon_3=(2n+\zeta)\sqrt{1+\lambda_1}$ and $b=\frac{1}{k}+H_\alpha^2$.

$P(\zeta,t)$ can be obtained by applying the inverse LT on the above equation

$$P(\zeta,t)=e^{-(2n-\zeta)\sqrt{\Upsilon_2}}=\sum_{n=0}^{\infty}\sum_{k=0}^{\infty}\frac{(-\Upsilon_3)^k}{k!}\sum_{l=0}^{\infty}\frac{\Gamma\left(\frac{k}{2}+1\right)}{\left(\frac{k}{2}-l+1\right)}\left(\frac{1}{\lambda}\right)^{\frac{k}{2}-m}\left(b-\frac{1}{\lambda}\right)^l\sum_{p=0}^{\infty}(-1)^p\frac{\Gamma(l+p)}{p!\Gamma l}\lambda^p\frac{t^{-\eta p+1}}{\Gamma(-\eta p)}. \tag{45}$$

Here,

$$Q(\zeta,q) = e^{-(2n+\zeta)\sqrt{\Upsilon_2}} = \sum_{n=0}^{\infty}\sum_{k=0}^{\infty}\frac{(-\Upsilon_4)^k}{k!}\sum_{l=0}^{\infty}\frac{\Gamma\left(\frac{k}{2}+1\right)}{\left(\frac{k}{2}-l+1\right)}\left(\frac{1}{\lambda}\right)^{\frac{k}{2}-l}\left(b-\frac{1}{\lambda}\right)^{l}\sum_{p=0}^{\infty}(-1)^p\frac{\Gamma(l+p)}{p!\Gamma l}\lambda^p q^{\eta p}, \tag{46}$$

where $\Upsilon_3 = (2n+2-\zeta)\sqrt{1+\lambda_1}$ and $b = \frac{1}{k}+H_\alpha^2$.

Applying the inverse LT on the above equation

$$Q(\zeta,t) = e^{-(2n-\zeta)\sqrt{\Upsilon_2}} = \sum_{n=0}^{\infty}\sum_{k=0}^{\infty}\frac{(-\Upsilon_4)^k}{k!}\sum_{l=0}^{\infty}\frac{\Gamma\left(\frac{k}{2}+1\right)}{\left(\frac{k}{2}-l+1\right)}\left(\frac{1}{\lambda}\right)^{\frac{k}{2}-l}\left(b-\frac{1}{\lambda}\right)^{l}\sum_{p=0}^{\infty}(-1)^p\frac{\Gamma(l+p)}{p!\Gamma l}\lambda^p\frac{t^{-\eta p+1}}{\Gamma(-\eta p)}. \tag{47}$$

Keeping in view Eqs (45) and (47) and implementing the inverse LT on Eq. (43), the expression obtained for $\omega_1(\zeta,t)$ is as stated below

$$\omega_1(\zeta,t) = f(t) * \big(P(\zeta,t) - Q(\zeta,t)\big). \tag{48}$$

and $\omega_2(\zeta,q)$ is expressed as

$$\omega_2(\zeta,q) = \frac{G_r}{q\Upsilon_0(P_r q^n - \Upsilon_2)sinh\sqrt{\Upsilon_2}}\Big(qG(q)\sinh\big((1-\zeta)\sqrt{\Upsilon_2}\big) - \sinh\big(\zeta\sqrt{\Upsilon_2}\big)\Big) \tag{49}$$

The simplified form of the expression $\omega_2(\zeta,q)$ is

$$\omega_2(\zeta,q) = G_r(1+\lambda_1)I(\zeta,q)\big((qG(q)R(\zeta,q) - (\zeta,q)\big), \tag{50}$$

where

$$I(\zeta,q) = \frac{1}{(P_r q^n(1+\lambda q^n) - (q^n+b)(1+\lambda_1))}, \tag{51}$$

and its inverse LT

$$I(\zeta,q) = -\sum_{n=0}^{\infty}\sum_{n=0}^{\infty}\frac{{a_0}^{n-k}{b_0}^{k}}{{c_0}^{n+1}}\frac{n!}{k!(n-k)!}\frac{t^{\eta(k-2n)-1}}{\Gamma_n(k-2n)}, \tag{52}$$

$where\ a_0 = P_r\lambda,\ b_0 = P_r - 1 - \lambda_1,\ c_0 = b(1+\lambda_1)$.

Here,

$$R(\zeta,q) = \frac{sinh\big((1-\zeta)\sqrt{\Upsilon_2}\big)}{qsinh\sqrt{\Upsilon_2}}, \tag{53}$$

$$R(\zeta,q) = \frac{sinh\big(\zeta\sqrt{\Upsilon_2}\big)}{qsinh\sqrt{\Upsilon_2}}, \tag{54}$$

Inverse LT on Eqs (53) and (54) is stated below as

$$R(\zeta,t) = \sum_{n=0}^{\infty}\sum_{k=0}^{\infty}\frac{\big((-\Upsilon_3)^k - (-\Upsilon_4)^k\big)}{n!}\sum_{l=0}^{\infty}\frac{\Gamma\left(\frac{k}{2}+1\right)}{\left(\frac{k}{2}-l+1\right)}\left(\frac{1}{\lambda}\right)^{\frac{k}{2}-m}\left(b-\frac{1}{\lambda}\right)^{l}\sum_{p=0}^{\infty}(-1)^p\frac{\Gamma(l+p)}{p!\Gamma l}\lambda^p\frac{t^{-\eta p+1}}{\Gamma(-\eta p)}, \tag{55}$$

where

$\Upsilon_3 = (2n+\zeta)\sqrt{1+\lambda_1}$ and $\Upsilon_4 = (2n+2-\zeta)\sqrt{1+\lambda_1}$

$$S(\zeta,t) = \sum_{n=0}^{\infty}\sum_{k=0}^{\infty}\frac{\big((-\Upsilon_5)^k - (-\Upsilon_6)^k\big)}{n!}\sum_{l=0}^{\infty}\frac{\Gamma\left(\frac{k}{2}+1\right)}{\left(\frac{k}{2}-l+1\right)}\left(\frac{1}{\lambda}\right)^{\frac{k}{2}-m}\left(b-\frac{1}{\lambda}\right)^{l}\sum_{p=0}^{\infty}(-1)^p\frac{\Gamma(l+p)}{p!\Gamma l}\lambda^p\frac{t^{-\eta p+1}}{\Gamma(-\eta p)}, \tag{56}$$

$\Upsilon_5 = (2n+1+\zeta)\sqrt{1+\lambda_1}$ and $\Upsilon_6 = (2n+1+\zeta)\sqrt{1+\lambda_1}$

Applying the inverse LT in Eq. (50)

$$\omega_2(\zeta,t) = G_r(1+\lambda_1)I(\zeta,t) * \Big(g'(t) * R(\zeta,t) - S(\zeta,t)\Big), \tag{57}$$

where we get the values of $I(\zeta,t)$, $R(\zeta,t)$ and $S(\zeta,t)$ from Eq. (52), Eq. (55) and Eq. (56) respectively.

Let us consider now

$$\omega_3(\zeta,t) = \frac{G_r}{q\Upsilon_0(P_r q^n - \Upsilon_2)sinh\sqrt{P_r q^n}}\Big(qG(q)\sinh\big((1-\zeta)\sqrt{P_r q^n}\big) - \sinh\big(\zeta\sqrt{P_r q^n}\big)\Big) = \frac{G_r(1+\lambda_1)}{(P_r q^n(1+\lambda q^n) - (q^n+b)(1+\lambda_1))} * \left(\frac{qG(q)sinh(1-\zeta)\sqrt{P_r q^n} - sinh\big(\zeta\sqrt{P_r q^n}\big)}{qsinh\sqrt{P_r q^n}}\right) \tag{58}$$

In simplest form $\omega_3(\zeta,q)$ is expressed as

$$\omega_3(\zeta,q) = G_r(1+\lambda_1)I(\zeta,q)\big(q(G(q)\vartheta_1(\zeta,q) - \vartheta_2(\zeta,q)\big), \tag{59}$$

and its inverse LT expression as

$$\omega_3(\zeta,q) = G_r(1+\lambda_1)I(\zeta,q) * \Big(g'(t) * \vartheta_1(\zeta,q) - \vartheta_2(\zeta,q)\Big), \tag{60}$$

where $I(\zeta,q)$, $\vartheta_1(\zeta,q)$, $\vartheta_2(\zeta,q)$ are expressed in Eqs (52), (25), and (27), respectively.

Now consider,

$$\omega_4(\zeta,q) = \frac{G_c}{q\Upsilon_0(S_c q^n - \Upsilon_2)sinh\sqrt{\Upsilon_2}}\Big(qH(q)\sinh\big((1-\zeta)\sqrt{\Upsilon_2}\big) - \sinh\big(\zeta\sqrt{\Upsilon_2}\big)\Big) = \frac{G_c(1+\lambda_1)}{(S_c q^n(1+\lambda q^n) - (q^n+b)(1+\lambda_1))} * \left(\frac{qH(q)sinh(1-\zeta)\sqrt{\Upsilon_2} - sinh\big(\zeta\sqrt{\Upsilon_2}\big)}{qsinh\sqrt{\Upsilon_2}}\right). \tag{61}$$

$$\omega_4(\zeta,q) = G_c(1+\lambda_1)J(\zeta,q)\big(q(H(q)R(\zeta,q) - S(\zeta,q)\big), \tag{62}$$

where

$$J(\zeta,q) = \frac{1}{(S_c q^n(1+\lambda q^n) - (q^n+b)(1+\lambda_1))}. \tag{63}$$

Implementing the LT in EQ. (63) gives

$$J(\zeta,t) = -\sum_{n=0}^{\infty}\sum_{k=0}^{\infty}\frac{d_0^{n-k}e_0^k}{c_0^{n+1}}\frac{t^{\eta(k-2n)-1}}{\Gamma_\eta(k-2n)}, \tag{64}$$

where $d_0 = S_c\lambda,\ e_0 = S_c - 1 - \lambda_1,\ c_0 = b(1+\lambda_1)$.

The $\omega_4(\zeta,q)$ expression takes the form

$$\omega_4(\zeta,t) = G_c(1+\lambda_1)J(\zeta,t) * \Big(h'(t) * R(\zeta,t) - S(\zeta,t)\Big), \tag{65}$$

where we get the values of $J(\zeta,t)$, $R(\zeta,t)$ and $S(\zeta,t)$ from Eqs (64), (55) and (56), respectively.

$$\omega_5(\zeta,q) = \frac{G_c}{q\Upsilon_0(S_c q^n - \Upsilon_2)sinh\sqrt{S_c q^n}}\Big(qH(q)\sinh\big((1-\zeta)\sqrt{S_c q^n}\big) - \sinh\big(\zeta\sqrt{S_c q^n}\big)\Big) = \frac{G_r(1+\lambda_1)}{(S_c q^n(1+\lambda q^n) - (q^n+b)(1+\lambda_1))} * \left(\frac{qG(q)sinh(1-\zeta)\sqrt{S_c q^n} - sinh\big(\zeta\sqrt{S_c q^n}\big)}{qsinh\sqrt{P_r q^n}}\right) \tag{66}$$

In simplest form, we can write it as

$$\omega_5(\zeta,q)=G_c(1+\lambda_1)J(\zeta,q)\big(q(H(q)\phi_1(\zeta,q)-\phi_2(\zeta,q)\big), \tag{67}$$

And its inverse LT

$$\omega_5(\zeta,q)=G_c(1+\lambda_1)J(\zeta,t)*\left(h'(t)*\phi_1(\zeta,t)-\phi_2(\zeta,t)\right), \tag{68}$$

where $J(\zeta,t),\phi_1(\zeta,t),\phi_2(\zeta,t)$ are obtained in Eqs (64), (33) and (35), respectively.

Introducing the expression of $\omega_1(\zeta,t)$, $\omega_2(\zeta,t)$, $\omega_3(\zeta,t)$, $\omega_4(\zeta,t)$, $\omega_5(\zeta,t)$ from Eqs (48), (57), (60), (65) and (68), respectively, into Eq. (41) after implementing the LT, the exact velocity solution is achieved as

$$\omega(\zeta,t)=\omega_1(\zeta,t)+\omega_2(\zeta,t)-\omega_3(\zeta,t)+\omega_4(\zeta,t)-\omega_5(\zeta,t) \tag{69}$$

The solution obtained for velocity in Eq. (69) (with $G_c=0$) is similar to the solution attained in literature [40].

4.2. Caputo Fabrizio formulation and solution

Replace the time deriavtive with the CF fractional derivative into Eqs (9)–(11) as,

$$^{CF}D_t^{\eta}\omega(\zeta,t)=\frac{1}{1+\lambda_1}\left(1+\lambda\,^{CF}D_t^{\eta}\right)\frac{\partial^2\omega(\zeta,t)}{\partial\zeta^2}-\left(\frac{1}{K}+H_a^2\right)\omega(\zeta,t)+G_r\vartheta(\zeta,t)+G_c\Phi(\zeta,t), \tag{70}$$

$$P_r\,^{CF}D_t^{\eta}\vartheta(\zeta,t)=\frac{\partial^2\omega(\zeta,t)}{\partial\zeta^2}, \tag{71}$$

$$S_c\,^{CF}D_t^{\eta}\Phi(\zeta,t)=\frac{\partial^2\Phi(\zeta,t)}{\partial\zeta^2}, \tag{72}$$

4.2.1 Investigation of exact solution of for temperature profile

By introducing the LT into Eq. (71) we get

$$\frac{\partial^2\overline{\vartheta}(\zeta,q)}{\partial\zeta^2}-\frac{P_r q z_0}{q+\gamma}\overline{\vartheta}(\zeta,q)=0, \tag{73}$$

where $z_0=\frac{1}{1-\eta},\gamma=\eta z_0$ and $\overline{\vartheta}(\zeta,q)$ meets the prescribed conditions below

$$\overline{\vartheta}(0,q)=G(q),\overline{\vartheta}(1,q)=\frac{1}{q}. \tag{74}$$

The implementation of prescribed boundary conditions Eq. (74) on solving the above differential equations produce the solution

$$\overline{\vartheta}(\zeta,q)=qG(q)\left(\frac{\sinh\left((1-\zeta)\sqrt{\frac{P_r z_0 q}{q+\gamma}}\right)}{q\sinh\left(\sqrt{\frac{P_r z_0 q}{q+\gamma}}\right)}\right)+\left(\frac{\sinh\left(\zeta\sqrt{\frac{P_r z_0 q}{q+\gamma}}\right)}{q\sinh\left(\sqrt{\frac{P_r z_0 q}{q+\gamma}}\right)}\right)=gG(q)\vartheta_1(\zeta,q)+\vartheta_2(\zeta,q). \tag{75}$$

The expression of $\vartheta_1(\zeta,t),\vartheta_2(\zeta,t)$ after employing the inverse LT on $\vartheta_1(\zeta,q),\vartheta_2(\zeta,q)$ respectively, is

$$\vartheta_1(\zeta,t)=\sum_{n=0}^{\infty}\sum_{k=1}^{\infty}\frac{(-\Xi_0)^k-(-\Xi_1)^k}{k!}*\sum_{m=0}^{\infty}\frac{\frac{k}{2!}}{m!\left(\frac{k}{2}-m\right)!}(-1)^m*\sum_{p=0}^{\infty}(-1)^p\frac{(m+p-1)!}{p!(m-1)!}\gamma^{-p}\frac{t^{-p}}{\Gamma(-p+1)} \tag{76}$$

where $\Xi_0=(2n+\zeta)\sqrt{P_r z_0}$ and $\Xi_1=(2n+2-\zeta)\sqrt{P_r z_0}$.

$$\vartheta_2(\zeta,t)=\sum_{n=0}^{\infty}\frac{2P_r}{\pi}\int_0^{\infty}\left(\frac{\sin\left(\frac{2n+1+\zeta}{\sqrt{1-\eta}}x\right)-\sin\left(\frac{2n+1-\zeta}{\sqrt{1-\eta}}x\right)}{x(P_r+x^2)}\right)e^{\frac{-\eta}{1-\eta}tx^2}dx. \tag{77}$$

The inverse LT of Eq. (75) is

$$\vartheta(\zeta,t)=\int_0^t g'(t-\tau)\vartheta_1(\zeta,\tau)d\tau+\vartheta_2(\zeta,t), \tag{78}$$

where $\vartheta_1(\zeta,t)$ and $\vartheta_2(\zeta,t)$ are expressed in Eqs (77) and (78), respectively.

4.2.2 Investigation of exact solution for concentration profile

Implement the LT into Eq. (72), and on solving we get

$$\frac{\partial^2\overline{\Phi}(\zeta,q)}{\partial\zeta^2}-\frac{S_c q z_0}{q+\gamma}\overline{\Phi}(\zeta,q)=0, \tag{79}$$

where $z_0=\frac{1}{1-\eta},\gamma=\eta z_0$ and $\overline{\Phi}(\zeta,q)$ satisfies the prescribed conditions

$$\overline{\Phi}(0,q)=H(q),\overline{\Phi}(1,q)=\frac{1}{q} \tag{80}$$

The implementation of the prescribed boundary conditions Eq. (80) on solving the above differential equations produce the solution of concentration as

$$\overline{\Phi}(\zeta,q)=qH(q)\left(\frac{\sinh\left((1-\zeta)\sqrt{\frac{S_c z_0 q}{q+\gamma}}\right)}{q\sinh\left(\sqrt{\frac{S_c z_0 q}{q+\gamma}}\right)}\right)+\left(\frac{\sinh\left(\zeta\sqrt{\frac{S_c z_0 q}{q+\gamma}}\right)}{q\sinh\left(\sqrt{\frac{S_c z_0 q}{q+\gamma}}\right)}\right)=gH(q)\Phi_1(\zeta,q)+\Phi_2(\zeta,q). \tag{81}$$

Employ the inverse LT on $\Phi_1(\zeta,q)$

$$\Phi_1(\zeta,q)=\sum_{n=0}^{\infty}\sum_{k=1}^{\infty}\frac{(-\Xi_0)^k-(-\Xi_1)^k}{k!}*\sum_{m=0}^{\infty}\frac{\frac{k}{2!}}{m!\left(\frac{k}{2}-m\right)!}(-1)^m*\sum_{p=0}^{\infty}(-1)^p\frac{(m+p-1)!}{p!(m-1)!}\gamma^{-p}\frac{t^{-p}}{\Gamma(-p+1)} \tag{82}$$

where $\Xi_0=(2n+\zeta)\sqrt{S_c z_0}$ and $\Xi_1=(2n+2-\zeta)\sqrt{S_c z_0}$.

Implementing the inverse LT on $\Phi_2(\zeta,q)$

$$\Phi_2(\zeta,q)=\sum_{n=0}^{\infty}\frac{2S_c}{\pi}\int_0^{\infty}\left(\frac{\sin\left(\frac{2n+1+\zeta}{\sqrt{1-\eta}}x\right)-\sin\left(\frac{2n+1-\zeta}{\sqrt{1-\eta}}x\right)}{x(S_c+x^2)}\right)e^{\frac{-\eta}{1-\eta}tx^2}dx. \tag{83}$$

Taking inverse LT in Eq. (81), we will get the expression of $\Phi(\zeta,t)$

$$\Phi(\zeta,t)=\int_0^t h'(t-\tau)\Phi_1(\zeta,\tau)d\tau+\Phi_2(\zeta,t), \quad (84)$$

where $\Phi_1(\zeta,t)$ and $\Phi_2(\zeta,t)$ are expressed in Eqs (82) and (83), respectively.

4.2.3 Investigation of exact solution for velocity profile

Applying the LT in Eq. (70), using the LT formula for CF derivative and bearing in mind the corresponding initial condition, we get

$$\left(\frac{qz_1+\gamma}{(1+\lambda_1)(q+\gamma)}\right)\frac{\partial^2\overline{\omega}(\zeta,q)}{\partial\zeta^2}-\left(\frac{qz_0}{q+\gamma}+\frac{1}{K}+H_a^2\right)\overline{\omega}(\zeta,q)=-G_r\overline{\vartheta}(\zeta,q)=-G_c\overline{\Phi}(\zeta,q), \quad (85)$$

$$\frac{\partial^2\overline{\omega}(\zeta,q)}{\partial\zeta^2}-\Lambda_2\overline{\omega}(\zeta,q)=\frac{-G_r}{\Lambda_0}\overline{\vartheta}(\zeta,q)-\frac{-G_c}{\Lambda_0}\overline{\Phi}(\zeta,q), \quad (86)$$

where $z_0=\frac{1}{1-\eta}, z_1=1+\lambda z_0, \Lambda_0=\left(\frac{qz_1+\gamma}{(1+\lambda_1)(q+\gamma)}\right), \Lambda_1=\left(\frac{qz_0}{q+\gamma}+\frac{1}{K}+H_a^2\right)$ and $\Lambda_2=\frac{\Lambda_1}{\Lambda_0}$.

The boundary conditions after embedding the LT are

$$\overline{\omega}=(0,q)=F(q), \overline{\omega}=(1,q)=0. \quad (87)$$

After inserting Eq. (75) into Eq. (86), the solution for Eq. (81) is obtained as

$$\begin{aligned}\overline{\omega}(\zeta,q)&=\frac{F(q)}{\sinh\sqrt{\Lambda_2}}\sinh\left((1-\zeta)\sqrt{\Lambda_2}\right)\\&+\frac{G_r}{q\Lambda_0\left(\frac{P_rz_0q}{q+\gamma}-\Lambda_2\right)\sinh\sqrt{\Lambda_2}}\left(qG(q)\sinh\left((1-\zeta)\sqrt{\Lambda_2}\right)-\sinh\left(\zeta\sqrt{\Lambda_2}\right)\right)-\\&\frac{G_r}{q\Lambda_0\left(\frac{P_rz_0q}{q+\gamma}-\Lambda_2\right)\sinh\sqrt{\frac{P_rz_0q}{q+\gamma}}}\left(qG(q)\sinh\left((1-\zeta)\sqrt{\frac{P_rz_0q}{q+\gamma}}\right)-\sinh\left(\zeta\sqrt{\frac{P_rz_0q}{q+\gamma}}\right)\right)+\\&\frac{G_c}{q\Lambda_0\left(\frac{S_cz_0q}{q+\gamma}-\Lambda_2\right)\sinh\sqrt{\Lambda_2}}\left(qH(q)\sinh\left((1-\zeta)\sqrt{\Lambda_2}\right)-\sinh\left(\zeta\sqrt{\Lambda_2}\right)\right)-\\&\frac{G_c}{q\Lambda_0\left(\frac{S_cz_0q}{q+\gamma}-\Lambda_2\right)\sinh\sqrt{\frac{S_cz_0q}{q+\gamma}}}\left(qH(q)\sinh\left((1-\zeta)\sqrt{\frac{S_cz_0q}{q+\gamma}}\right)-\sinh\left(\zeta\sqrt{\frac{S_cz_0q}{q+\gamma}}\right)\right).\end{aligned} \quad (88)$$

For suitable presentation of velocity equation, we rewrite Eq. (88) into the following simplified form

$$\overline{\omega}(\zeta,q)=\omega_1(\zeta,q)+\omega_2(\zeta,q)-\omega_3(\zeta,q)+\omega_4(\zeta,q)-\omega_5(\zeta,q), \quad (89)$$

where

$$\omega_1(\zeta,q)=\frac{F(q)}{\sinh\sqrt{\Lambda_2}}\sinh\left((1-\zeta)\sqrt{\Lambda_2}\right)=F(q)L(\zeta,q). \quad (90)$$

Employing the inverse LT on $L(\zeta,q)$, we arrived at

$$L(\zeta,t)=\sum_{n=0}^{\infty}\sum_{k=0}^{\infty}\frac{\left((-\Xi_4)^k-(-\Xi_5)^k\right)}{k!}(1+\lambda_1)^{\frac{k}{2}}\sum_{m=0}^{\infty}\frac{\frac{k}{2}!}{m!\left(\frac{k}{2}-m\right)!}(z_3)^{\frac{k}{2}-m}(z_4)^m\times\sum_{p=0}^{\infty}(-1)^p\frac{(m+p-1)!}{p!(m-1)!}\gamma^{-(m+p)}(z_1)^p\frac{t^{-(p+1)}}{\Gamma(-p)} \quad (91)$$

where $b=\frac{1}{k}+H_a^2, z_0=\frac{1}{1-\eta}, z_1=1+\lambda z_0, z_2=z_0+b, z_3=\frac{z_2}{z_1}, z_4=\gamma(b-z_3), \Xi_0=(2n+\zeta)$ and $\Xi_1=(2n+2-\zeta)$.

Implementing the inverse LT of Eq. (90) while bearing in mind Eq. (91), we obtain

$$\omega_1(\zeta,t)=f(t)*L(\zeta,t). \quad (92)$$

The expression of $\omega_2(\zeta,q)$ is

$$\omega_2(\zeta,q)=\frac{G_r}{q\Lambda_0\left(\frac{P_rz_0q}{q+\gamma}-\Lambda_2\right)\sinh\sqrt{\Lambda_2}}\left(qG(q)\sinh\left((1-\zeta)\sqrt{\Lambda_2}\right)-\sinh\left(\zeta\sqrt{\Lambda_2}\right)\right), \quad (93)$$

and in the simplest form

$$\omega_2(\zeta,q)=G_r(1+\lambda_1)I_1(\zeta,q)\left(qG(q)R_1(\zeta,q)-S_1(\zeta,q)\right) \quad (94)$$

where

$$I_1(\zeta,q)=\frac{1}{\left(P_rz_0q(qz_1+\gamma)-(qz_2+b\gamma)(q+\gamma)(1+\lambda_1)\right)}, \quad (95)$$

And its inverse LT is

$$I_1(\zeta,t)=-\sum_{n=0}^{\infty}\sum_{k=0}^{\infty}\frac{f_0^{n-k}g_0^k}{h_0^{n+1}}\frac{n!}{k!(n-k)!}\frac{t^{\eta(k-2n)-1}}{\Gamma\eta(k-2n)}, \quad (96)$$

where $f_0=\left(P_rz_0z_1-z_2(1+\lambda_1)\right)$, $g_0=\left(P_rz_0\gamma-z_2(1+\lambda_1)-b\gamma(1+\lambda_1)\right), h_0=b\gamma^2(1+\lambda_1)$

$$R_1(\zeta,q)=\frac{(q+\gamma)^2\sinh\left((1-\zeta)\sqrt{\Lambda_2}\right)}{q\sinh\sqrt{\Lambda_2}}, \quad (97)$$

$$S_1(\zeta,q)=\frac{(q+\gamma)^2\sinh\left(\zeta\sqrt{\Lambda_2}\right)}{q\sinh\sqrt{\Lambda_2}}. \quad (98)$$

Inverse LT in Eqs (97) and (98) is transformed into

$$R_1(\zeta,q)=\sum_{\beta=0}^{2}\frac{2!}{\beta!(2-\beta)!}\sum_{n=0}^{\infty}\sum_{k=0}^{\infty}\frac{\left((-\Xi_4)^k-(-\Xi_5)^k\right)}{k!}(1+\lambda_1)^{\frac{k}{2}}\sum_{m=0}^{\infty}\frac{\frac{k}{2}!}{m!\left(\frac{k}{2}-m\right)!}(z_3)^{\frac{k}{2}-m}(z_4)^m\times\sum_{p=0}^{\infty}(-1)^p\frac{(m+p-1)!}{p!(m-1)!}\gamma^{-(m+p+\beta-2)}(z_1)^p\frac{t^{-(\beta+p)}}{\Gamma(-(\beta+p)+1)}, \quad (99)$$

$$S_1(\zeta,q)=\sum_{\beta=0}^{2}\frac{2!}{\beta!(2-\beta)!}\sum_{n=0}^{\infty}\sum_{k=0}^{\infty}\frac{\left((-\Xi_6)^k-(-\Xi_7)^k\right)}{k!}(1+\lambda_1)^{\frac{k}{2}}\sum_{m=0}^{\infty}\frac{\frac{k}{2}!}{m!\left(\frac{k}{2}-m\right)!}(z_3)^{\frac{k}{2}-m}(z_4)^m\times\sum_{p=0}^{\infty}(-1)^p\frac{(m+p-1)!}{p!(m-1)!}\gamma^{-(m+p+\beta-2)}(z_1)^p\frac{t^{-(\beta+p)}}{\Gamma(-(\beta+p)+1)}, \quad (100)$$

DOI 10.2478/ama-2023-0068

where $b=\frac{1}{k}+H_a^2$, $z_0=\frac{1}{1-\eta}$, $z_1=1+\lambda z_0$, $z_2=z_0+b$, $z_3=\frac{z_2}{z_1}$, $z_4=\gamma(b-z_3)$, $\Xi_4=(2n+\zeta)$ and $\Xi_5=(2n+2-\zeta)$, $\Xi_6=(2n+1-\zeta)$ and $\Xi_7=(2n+1+\zeta)$.

The $\omega_2(\zeta,t)$ is expressed as

$$\omega_2(\zeta,t)=G_r(1+\lambda_1)I_1(\zeta,t)*\big(g'(t)*R_1(\zeta,t)-S-1(\zeta,t)\big) \quad (101)$$

where we get the values of $I_1(\zeta,t),R_1(\zeta,t)$ and $S_1(\zeta,t)$ from Eqs (96), (99) and (100), respectively.

Consider now,

$$\omega_3(\zeta,q)=\frac{G_r}{q\Lambda_0\left(\frac{P_r z_0 q}{q+\gamma}-\Lambda_2\right)\sinh\sqrt{\frac{P_r z_0 q}{q+\gamma}}}\left(qG(q)\sinh\left((1-\zeta)\sqrt{\frac{P_r z_0 q}{q+\gamma}}\right)-\sinh\left(\zeta\sqrt{\frac{P_r z_0 q}{q+\gamma}}\right)\right) \quad (102)$$

And the abridged form

$$\omega_3(\zeta,q)=G_r(1+\lambda_1)I_1(\zeta,q)\big(qG(q)\varphi_1(\zeta,q)-\varphi_2(\zeta,q)\big). \quad (103)$$

Taking the inverse LT in Eq. (103)

$$\omega_3(\zeta,t)=G_r(1+\lambda_1)I_1(\zeta,t)*\big(g'(t)*\varphi_1(\zeta,t)-\varphi_2(\zeta,t)\big), \quad (104)$$

where $I_1(\zeta,t)$, is obtained in Eq. (96), and $\varphi_1(\zeta,t),\varphi_2(\zeta,t)$ are obtained as below

$$\varphi_1(\zeta,q)=\sum_{\beta=0}^{2}\frac{2!}{\beta!(2-\beta)!}\sum_{n=0}^{\infty}\sum_{k=0}^{\infty}\frac{\left((-\Xi_0)^k-(-\Xi_1)^k\right)}{k!}\sum_{m=0}^{\infty}\frac{\frac{k}{2}!}{m!\left(\frac{k}{2}-m\right)!}(-1)^m \sum_{p=0}^{\infty}(-1)^p\frac{(m+p-1)!}{p!(m-1)!}\gamma^{-(\beta+p-2)}(z_1)^p\frac{t^{-(\beta+p)}}{\Gamma(-(\beta+p)+1)}, \quad (105)$$

where $\Xi_2=(2n+\zeta)\sqrt{P_r z_0}$ and $\Xi_3=(2n+2-\zeta)\sqrt{P_r z_0}$, and

$$\varphi_1(\zeta,q)=\sum_{\beta=0}^{2}\frac{2!}{\beta!(2-\beta)!}\sum_{n=0}^{\infty}\sum_{k=0}^{\infty}\frac{\left((-\Xi_8)^k-(-\Xi_9)^k\right)}{k!}\sum_{m=0}^{\infty}\frac{\frac{k}{2}!}{m!\left(\frac{k}{2}-m\right)!}(-1)^m \times\sum_{p=0}^{\infty}(-1)^p\frac{(m+p-1)!}{p!(m-1)!}\gamma^{-(\beta+p-2)}(z_1)^p\frac{t^{-(\beta+p)}}{\Gamma(-(\beta+p)+1)}, \quad (106)$$

where $\Xi_8=(2n+1-\zeta)\sqrt{P_r z_0}$ and$\Xi_9=(2+1+\zeta)\sqrt{P_r z_0}$.

Here,

$$\omega_4(\zeta,q)=\frac{G_c}{q\Lambda_0\left(\frac{S_c z_0 q}{q+\gamma}-\Lambda_2\right)\sinh\sqrt{\Lambda_2}}\left(qH(q)\sinh\left((1-\zeta)\sqrt{\Lambda_2}\right)-\sinh\left(\zeta\sqrt{\Lambda_2}\right)\right), \quad (107)$$

which can be written in abridged form as

$$\omega_4(\zeta,q)=G_r(1+\lambda_1)J_1(\zeta,q)\big(qG(q)R_1(\zeta,q)-S_1(\zeta,q)\big), \quad (108)$$

where

$$J_1(\zeta,q)=\frac{1}{(S_c z_0 q(qz_1+\gamma)-(qz_2+b\gamma)(q+\gamma)(1+\lambda_1))} \quad (109)$$

And its inverse LT

$$J_1(\zeta,t)=-\sum_{n=0}^{\infty}\sum_{k=0}^{\infty}\frac{f_{01}^{n-k}g_{01}^{k}}{h_{01}^{n+1}}\frac{n!}{k!(n-k)!}\frac{t^{\eta(k-2n)-1}}{\Gamma\eta(k-2n)}, \quad (110)$$

where $f_{01}=\big(S_c z_0 z_1-z_2(1+\lambda_1)\big)$, $g_{01}=\big(S_c z_0\gamma-z_2(1+\lambda_1)-b\gamma(1+\lambda_1)\big)$, $h_{01}=b\gamma^2(1+\lambda_1)$,

The $\omega_4(\zeta,t)$ is expressed as

$$\omega_4(\zeta,t)=G_c(1+\lambda_1)J_1(\zeta,t)*\big(h'(t)*R_1(\zeta,t)-S_2(\zeta,t)\big), \quad (111)$$

where we get the values of $J_1(\zeta,t)$, $R_1(\zeta,t)$, $S_1(\zeta,t)$ from Eqs(110), (99) and (100), respectively.

The expression for $\omega_5(\zeta,q)$ is stated below as

$$\omega_4(\zeta,q)=\frac{G_c}{q\Lambda_0\left(\frac{S_c z_0 q}{q+\gamma}-\Lambda_2\right)\sinh\sqrt{\frac{S_c z_0 q}{q+\gamma}}}\left(qH(q)\sinh\left((1-\zeta)\sqrt{\frac{S_c z_0 q}{q+\gamma}}\right)-\sinh\left(\zeta\sqrt{\frac{S_c z_0 q}{q+\gamma}}\right)\right). \quad (112)$$

For simplification,

$$\omega_5(\zeta,t)=G_c(1+\lambda_1)J_1(\zeta,q)\big(qH(q)\psi_1(\zeta,q)-\psi_1(\zeta,q)\big), \quad (113)$$

and its inverse LT will take the form

$$(\zeta,t)=G_c(1+\lambda_1)J_1(\zeta,t)*\big(h'(t)*\psi_1(\zeta,t)-\psi_2(\zeta,t)\big), \quad (114)$$

where

$$\psi_1(\zeta,q)=\sum_{\beta=0}^{2}\frac{2!}{\beta!(2-\beta)!}\sum_{n=0}^{\infty}\sum_{k=0}^{\infty}\frac{\left((-\Xi_2)^k-(-\Xi_3)^k\right)}{k!}\times\sum_{m=0}^{\infty}\frac{\frac{k}{2}!}{m!\left(\frac{k}{2}-m\right)!}(-1)^m \times\sum_{p=0}^{\infty}(-1)^p\frac{(m+p-1)!}{p!(m-1)!}\gamma^{-(\beta+p-2)}(z_1)^p\frac{t^{-(\beta+p)}}{\Gamma(-(\beta+p)+1)}, \quad (115)$$

$$\psi_2(\zeta,q)=\sum_{\beta=0}^{2}\frac{2!}{\beta!(2-\beta)!}\sum_{n=0}^{\infty}\sum_{k=0}^{\infty}\frac{\left((-\Xi_{10})^k-(-\Xi_{11})^k\right)}{k!}\times\sum_{m=0}^{\infty}\frac{\frac{k}{2}!}{m!\left(\frac{k}{2}-m\right)!}(-1)^m \times\sum_{p=0}^{\infty}(-1)^p\frac{(m+p-1)!}{p!(m-1)!}\gamma^{-(\beta+p-2)}(z_1)^p\frac{t^{-(\beta+p)}}{\Gamma(-(\beta+p)+1)}, \quad (116)$$

where $\Xi_8=(2n+\zeta)\sqrt{S_c z_0}$ and $\Xi_{11}=(2+1+\zeta)\sqrt{S_c z_0}$.

Introducing the expression of $\omega_1(\zeta,t)$, $\omega_2(\zeta,t)$, $\omega_3(\zeta,t)$, $\omega_4(\zeta,t)$, $\omega_5(\zeta,t)$ from Eqs (92), (101), (104), (111) and (114), respectively, into Eq. (89), the velocity solution is attained as

$$\omega(\zeta,t)=\omega_1(\zeta,t)+\omega_2(\zeta,t)-\omega_3(\zeta,t)+\omega_4(\zeta,t)-\omega_5(\zeta,t). \quad (117)$$

sciendo
DOI 10.2478/ama-2023-0068 acta mechanica et automatica, vol.17 no.4 (2023)

5. LIMITING CASES OF MOMENTUM EQUATION

5.1. Velocity solution for second grade fluid

5.1.1 Caputo sense

Incorporating $\lambda_1 \to 0$, the velocity solution expressed in Eq. (40) transforms into the second-grade fluid solution

$$\overline{\omega}(\zeta,q)=\frac{F(q)}{sinh\sqrt{\Omega_2}}sinh\left((1-\zeta)\sqrt{\Upsilon_2}\right)+\frac{G_r}{q\Omega_0(P_rq^n-\Omega_2)sinh\sqrt{\Upsilon_2}}\left(qG(q)\sinh(1-\zeta)\sqrt{\Omega_2})-\sinh(\zeta\sqrt{\Omega_2})\right)-\frac{G_r}{q\Upsilon_0(P_rq^n-\Omega_2)sinh\sqrt{P_rq^n}}\left(qG(q)\sinh(1-\zeta)\sqrt{P_rq^n})-\sinh(\zeta\sqrt{P_rq^n})\right)+\frac{G_c}{q\Omega_0(S_cq^n-\Omega_2)sinh\sqrt{\Upsilon_2}}\left(qH(q)\sinh(1-\zeta)\sqrt{\Omega_2})-\sinh(\zeta\sqrt{\Omega_2})\right)-\frac{G_c}{q\Omega_0(S_cq^n-\Omega_2)sinh\sqrt{S_cq^n}}\left(qH(q)\sinh(1-\zeta)\sqrt{S_cq^n})-\sinh(\zeta\sqrt{S_cq^n})\right). \quad (118)$$

where $\Omega_0=1+\lambda q^n, \Omega_2=\frac{\lambda_1}{\Omega_0}$.

By taking $G_c=0$ in Eq. (118), the solution obtained is similar to the limiting solution attained by Asgir et al. [40]. For $\eta \to 1$, and resuming $G_c=0$, we will get the limiting result obtained by Aleem et al. [39].

5.2. Caputo Fabrizio sense

By taking $\lambda_1 \to 0$, the velocity solutions in Eq. (88) present the result of second-grade fluid

$$\overline{\omega}(\zeta,q)=\frac{F(q)}{\sinh\sqrt{\varrho_2}}\sinh\left((1-\zeta)\sqrt{\varrho_2}\right)+\frac{G_r}{q\varrho_0\left(\frac{P_rz_0q}{q+\gamma}-\varrho_2\right)\sinh\sqrt{\varrho_2}}\left(qG(q)\sinh\left((1-\zeta)\sqrt{\varrho_2}\right)-\sinh(\zeta\sqrt{\Lambda_2})\right)\frac{G_r}{q\varrho_0\left(\frac{P_rz_0q}{q+\gamma}-\varrho_2\right)\sinh\sqrt{\frac{P_rz_0q}{q+\gamma}}}\left(qG(q)\sinh\left((1-\zeta)\sqrt{\frac{P_rz_0q}{q+\gamma}}\right)-\sinh\left(\zeta\sqrt{\frac{P_rz_0q}{q+\gamma}}\right)\right)+\frac{G_c}{q\varrho_0\left(\frac{S_cz_0q}{q+\gamma}-\Lambda_2\right)\sinh\sqrt{\varrho_2}}\left(qH(q)\sinh\left((1-\zeta)\sqrt{\varrho_2}\right)-\sinh(\zeta\sqrt{\varrho_2})\right)-\frac{G_c}{q\varrho_0\left(\frac{S_cz_0q}{q+\gamma}-\Lambda_2\right)\sinh\sqrt{\frac{S_cz_0q}{q+\gamma}}}\left(qH(q)\sinh\left((1-\zeta)\sqrt{\frac{S_cz_0q}{q+\gamma}}\right)-\sinh\left(\zeta\sqrt{\frac{S_cz_0q}{q+\gamma}}\right)\right), \quad (119)$$

where $z_0=\frac{1}{1-\eta}$, $z_1=1+\lambda z_0$, $\varrho_0=\left(\frac{qz_1+\gamma}{(1+\lambda_1)(q+\lambda)}\right)$, $\Lambda_1=\left(\frac{qz_0}{q+\lambda}+\frac{1}{k}+H_\alpha^2\right)$, $\varrho_2=\frac{\Lambda_1}{\varrho_0}$. For $\eta \to 1$, the results recovered are of ordinary second-grade fluid. Further taking $G_c=0$, the results attained are similar to the limiting result of velocity [39].

5.3. Velocity solution for viscous fluid

5.3.1 Caputo sense

By introducing $\lambda \to 1, \lambda_1 \to 0$, and absence of porosity reduces the velocity solution of Jeffrey fluid into viscous fluid solution, which is stated as below

$$\overline{\omega}(\zeta,q)=\frac{F(q)}{\sinh\sqrt{q_n+H_\alpha^2}}\sinh\left((1-\zeta)\sqrt{q_n+H_\alpha^2}\right)++\frac{G_r}{q\left(P_rq^n-(q_n+H_\alpha^2)\right)sinh\sqrt{q_n+H_\alpha^2}}\left(qG(q)\,sinh\left((1-\zeta)\sqrt{q_n+H_\alpha^2}\right)-sinh\left(\zeta\sqrt{q_n+H_\alpha^2}\right)\right)-\frac{G_r}{q\left(P_rq^n-(q_n+H_\alpha^2)\right)sinh\sqrt{P_rq^n}}\left(qH(q)\,sinh\left((1-\zeta)\sqrt{P_rq^n}\right)-sinh\left(\zeta\sqrt{P_rq^n}\right)\right)+\frac{G_c}{q\left(S_cq^n-(q_n+H_\alpha^2)\right)sinh\sqrt{q_n+H_\alpha^2}}\left(qG(q)\,sinh\left((1-\zeta)\sqrt{q_n+H_\alpha^2}\right)-sinh\left(\zeta\sqrt{q_n+H_\alpha^2}\right)\right)-\frac{G_c}{q\left(S_cq^n-(q_n+H_\alpha^2)\right)sinh\sqrt{P_rq^n}}\left(qH(q)\,sinh\left((1-\zeta)\sqrt{P_rq^n}\right)-sinh\left(\zeta\sqrt{P_rq^n}\right)\right). \quad (120)$$

Further taking $G_c=0$, the results attained are similiar to the limiting result of velocity [40]. For $\eta \to 1$, and Gc = 0, we will attain the results for ordinary viscous fluid obtained by Aleem et al. [39].

5.3.2 Caputo Fabrizio sense

By introducing $\lambda \to 0, \lambda_1 \to 0$, in Eq. (88) and the absence of porosity presents the velocity solution of viscous fluid as below

$$\overline{\omega}(\zeta,q)=\frac{F(q)}{\sinh\sqrt{\frac{qz_0}{q+\gamma}+H_\alpha^2}}\sinh\left((1-\zeta)\sqrt{\frac{qz_0}{q+\gamma}+H_\alpha^2}\right)+\frac{G_r}{q\left(\frac{P_rz_0q}{q+\gamma}-\left(\frac{qz_0}{q+\gamma}+H_\alpha^2\right)\right)sinh\sqrt{\frac{qz_0}{q+\gamma}+H_\alpha^2}}\left(qG(q)\,sinh\left((1-\zeta)\sqrt{\frac{qz_0}{q+\gamma}+H_\alpha^2}\right)-sinh\left(\zeta\sqrt{\frac{qz_0}{q+\gamma}+H_\alpha^2}\right)\right)-\frac{G_r}{q\left(\frac{P_rz_0q}{q+\gamma}-\left(\frac{qz_0}{q+\gamma}+H_\alpha^2\right)\right)sinh\sqrt{\frac{P_rz_0q}{q+\gamma}}}\left(qG(q)\,sinh\left((1-\zeta)\sqrt{P_rq^n}\right)-sinh\left(\zeta\sqrt{P_rq^n}\right)\right)+\frac{G_c}{q\left(\frac{S_cz_0q}{q+\gamma}-\left(\frac{qz_0}{q+\gamma}+H_\alpha^2\right)\right)sinh\sqrt{\frac{qz_0}{q+\gamma}+H_\alpha^2}}\left(qG(q)\,sinh\left((1-\zeta)\sqrt{\frac{qz_0}{q+\gamma}+H_\alpha^2}\right)-sinh\left(\zeta\sqrt{\frac{qz_0}{q+\gamma}+H_\alpha^2}\right)\right)-\frac{G_c}{q\left(\frac{S_cz_0q}{q+\gamma}-\left(\frac{qz_0}{q+\gamma}+H_\alpha^2\right)\right)sinh\sqrt{\frac{S_cz_0q}{q+\gamma}}}\left(qH(q)\,sinh\left((1-\zeta)\sqrt{\frac{S_cz_0q}{q+\gamma}}\right)-sinh\left(\zeta\sqrt{\frac{S_cz_0q}{q+\gamma}}\right)\right), \quad (121)$$

where $z_0=\frac{1}{1-\eta}$. For $\eta \to 1$, we will attain the results for ordinary viscous fluid obtained by Aleem et al. [39].

DOI 10.2478/ama-2023-0068

6. GRAPHS AND DISCUSSION

The heat and mass transference study of MHD free convective flow of Jeffrey fluid bounded amidst two vertical plates via time-fractional C and CF is elaborated here. The flow phenomenon of the fluid happens owing to the moment of one plate while the other is kept constant. The dimensionless system of equations representing the fluid flow phenomenon is solved by the integral LT. The obtained results are presented in a series form. The graphical illustration is used to present the behaviour of embedded physical variables such as relaxation time, thermal Grashof number, permeability parameter, mass Grashof number, Schmidt number, Jeffrey fluid parameter Prandtl number and memory parameter on the temperature, concentration and velocity profile where the $F(q) = \frac{1}{q}, G(q) = \frac{1}{q^2}, H(q) = \frac{1}{q^2}$. Fig 2. manifests the temperature profile's fractional parameter control. As η increases, the boundary layer thickens, causing the temperature to rise. The boundary layer thickness elevates the heat of the particles. The finding for η → 1 is easily validated because it is already existing in the literature [39]. The concentration curves rise as well due to the same reason as shown in Fig. 5. The dominance of the mass diffusivity in fluid flow outcome is a reduction of the thermal boundary layer. The thermal boundary layer reduces, resulting in a decline in temperature. These are the effects of Pr which are elaborated in Fig. 3.

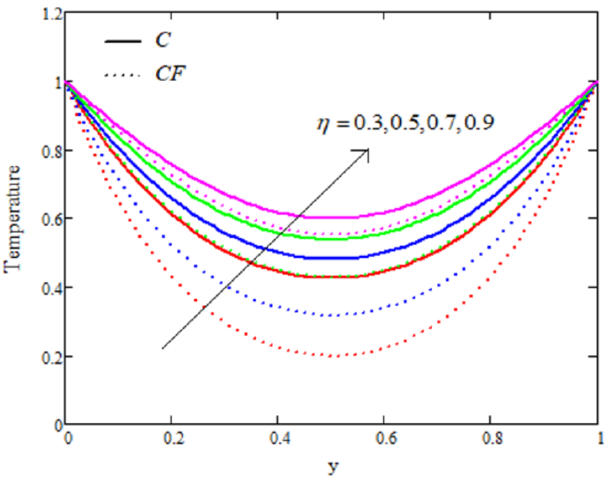

Fig. 2. Temperature plot for multiple values η with Pr = 5

The thermal boundary layer becomes thick with time, which results in an upgrade in temperature curves, as plotted in Fig. 4. We observed the similar impacts of time on the concentration profile graphed in Fig. 7. The govern of Sc on the concentration curves is depicted in Fig. 6. It is observed that the concentration descends with the rise in Sc values. Physically, this is true, because the Schmidt number increases and the concentration curves move towards the boundary, indicating the larger surface mass transfer.

The effect of the memory parameter η on fluid flow is depicted in Fig. 8. It is obvious that as η increases, so does the fluid velocity. The reason for this is that as η increases, so does the thickness of the boundary layer, resulting in velocity acceleration.

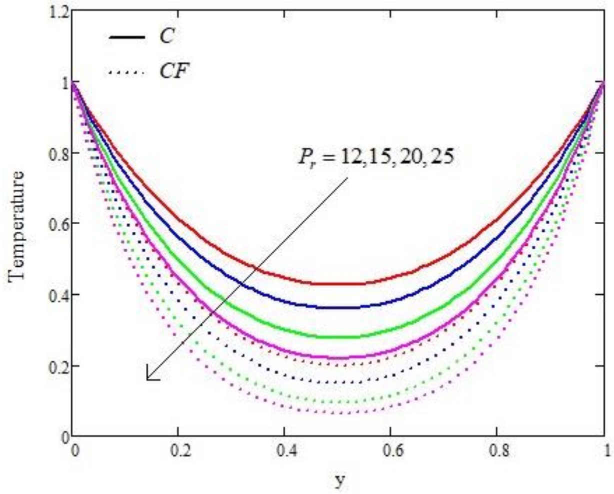

Fig. 3. Temperature plot for multiple values of Pr with η = 0.3

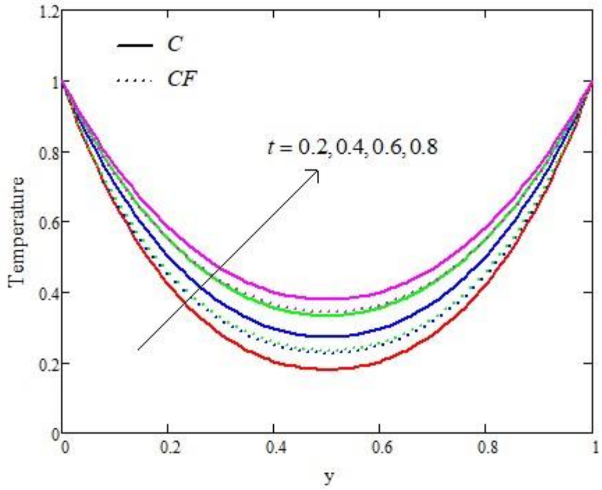

Fig. 4. Temperature plot for multiple values of t with Pr = 12 and η = 0.3

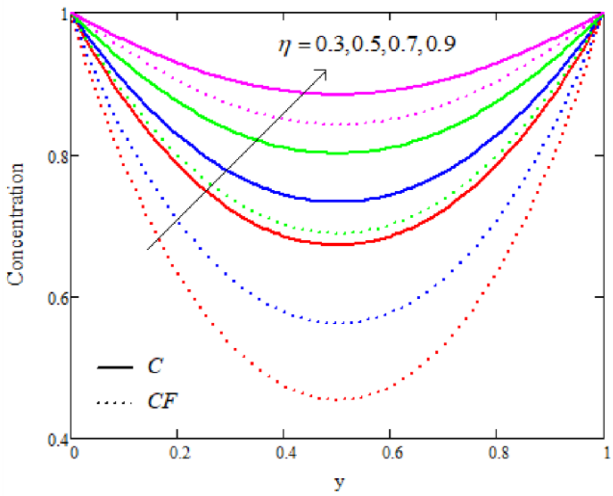

Fig. 5. Concentration plot for multiple values η with Sc = 5.0

DOI 10.2478/ama-2023-0068

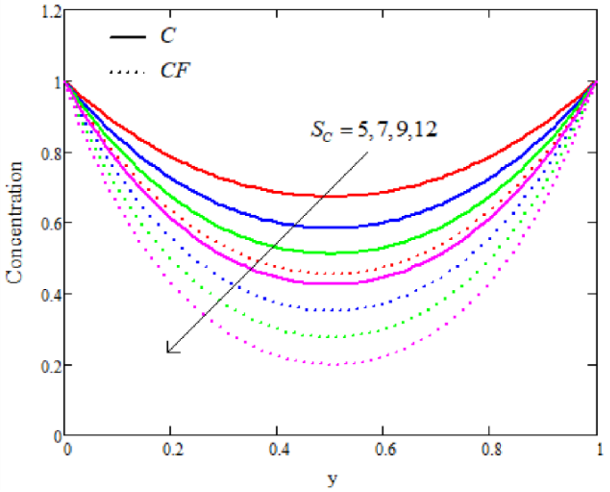

Fig. 6. Concentration plot for multiple values of Sc with η = 0.3

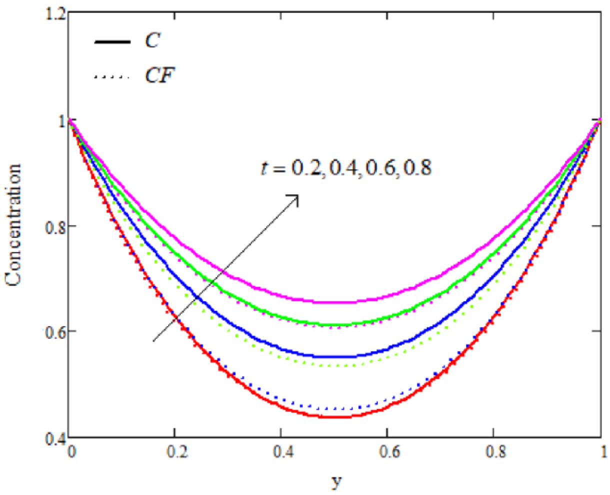

Fig. 7. Concentration plot for multiple values of t with Sc = 5.0 and η = 0.3

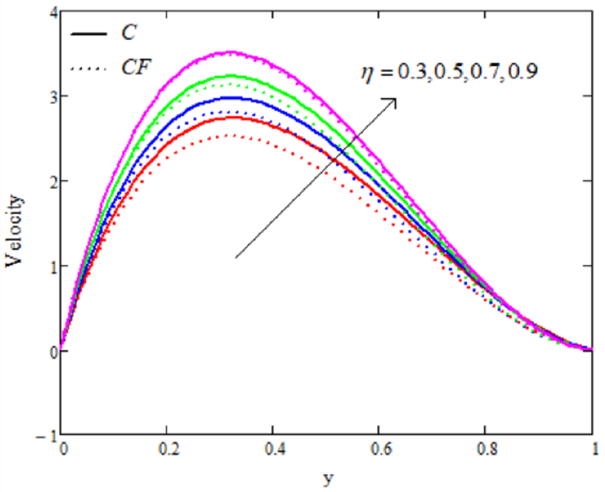

Fig. 8. Velocity plot for multiple values η with Gr = 5,Gc = 8,k = 0.2, Sc = 0.5,Ha = 0.3, λ = 0.9, λ1 =1.6,Pr = 7

The Prandtl number variation influence on the fluid flow is graphed in Fig. 9. From the figure, it is noted that higher Pr values reduce the velocity field. The thickness of the boundary layer was reduced with enhancement in the Prandtl number.

To elaborate on the effects of Gr, Fig. 10 is plotted. We observed that the fluid accelerates with the higher velocity with an ascent of thermal Grashof number Gr. Physically, increasing the value of Gr increases the buoyancy forces, which reduces the thickness of the momentum boundary layer and increases the velocity.

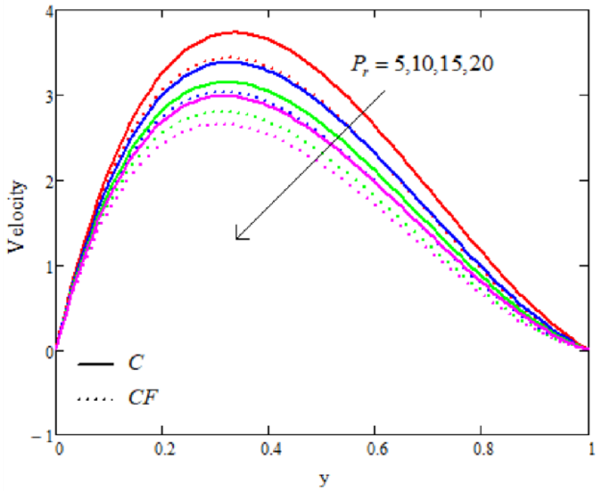

Fig. 9. Velocity plot for multiple values of P_r, Gr = 5,Gc = 8,k = 0.2, Sc = 0.5,Ha = 0.3,λ = 0.9, λ1 =1.6, η = 0.3

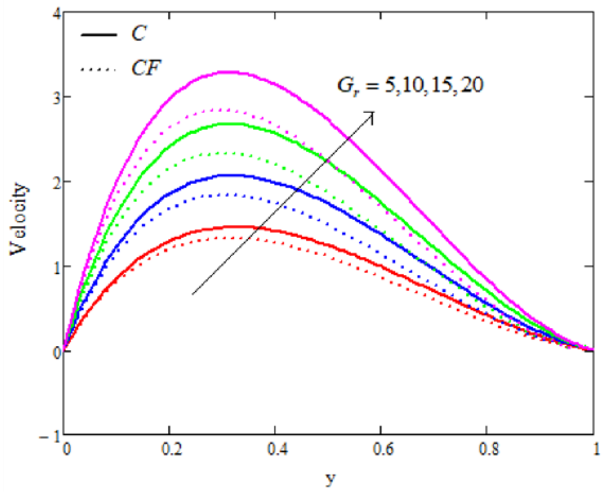

Fig. 10. Velocity plot for multiple values of Gr with Gc = 8,k = 0.2, Sc = 0.5,Ha = 0.3,λ = 0.9, λ1 =1.6, Pr = 7,η = 0.3

The velocity curves under the effect of mass Grashof number Gc can be observed in Fig. 11. It is observed that there is a rise in velocity curves with the ascent of mass Grashof number. This is true because the concentration gradient increases the buoyancy forces, and therefore velocity accelerates.

Fig.12 elucidates the impacts of the porosity on the fluid flow. An increment in the estimation of the porosity parameter diminishes the fluid flow speed. Resistive forces bring about a decline in the speed of fluid flow. Fig 13. portrays the impacts of Sc on the fluid flow. Adding up the value of the Sc results in descending velocity curves. The point to be observed is that higher values of the Schmidt number results in more viscosity in

DOI 10.2478/ama-2023-0068

fluid, causing a fall in the mass diffusion rate, and hence accordingly the fluid velocity diminishes.

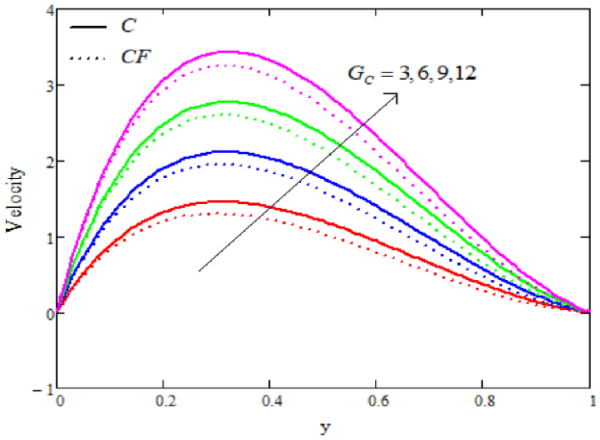

Fig. 11. Velocity plot for multiple values of Gc, with $G_r = 5$, k = 0.2,Sc.=0.5,Ha = 0.3,λ = 0.9,λ1 = $1.6, P_r = 7, \eta = 0.3$

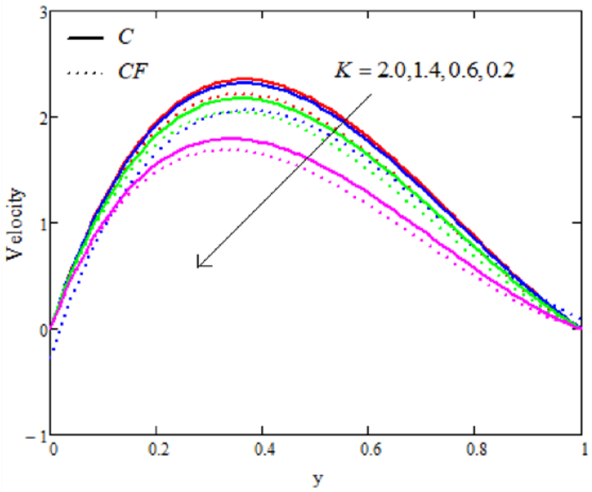

Fig. 12. Velocity plot for multiple values of K with with Gr = 5,Gc = 8, Sc = 0.5,Ha = 0.3,λ =0.9,λ1 = 1.6,Pr = 7,η = 0.3

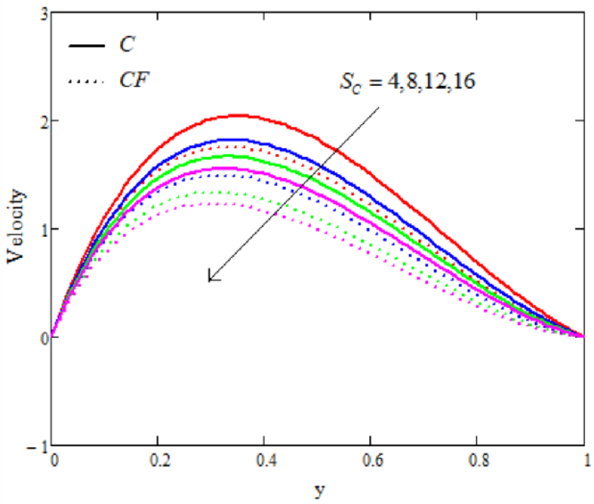

Fig. 13. Velocity plot for multiple values of S_c with $G_r = 5, G_c = 8$, $k = 0.2, H_a = 0.3, \lambda = 0.9, \lambda_1 = 1.6, P_r = 7, \eta = 0.3$

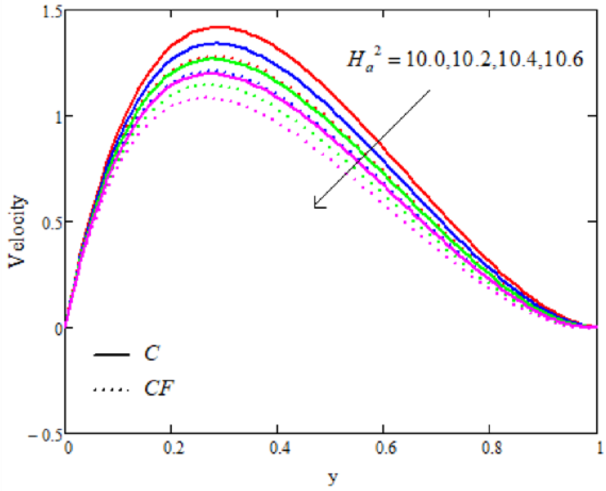

Fig. 14. Velocity plot for multiple values of Ha with Gr = 5,Gc = 8, k = 0.2,Sc = 0.5,λ = 0.9,λ1 = 1.6,Pr = 7,η = 0.3

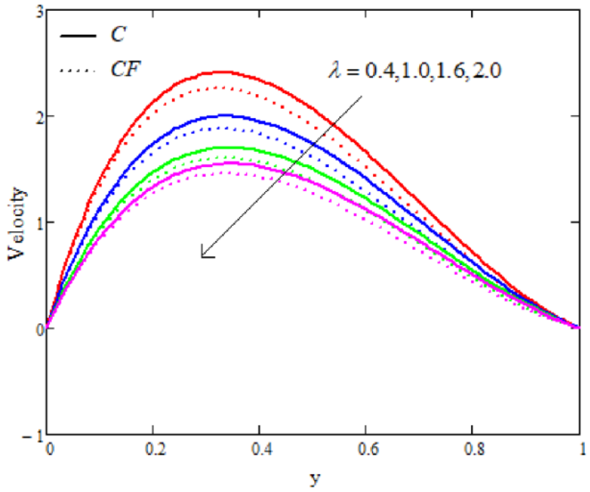

Fig. 15. Velocity plot for multiple values of λ with $G_r = 5, G_c = 8$, $k = 0.2, S_c\ 0.5, H_a = 0.3, \lambda_1 = 1.6, P_r = 7, \eta = 0.3$

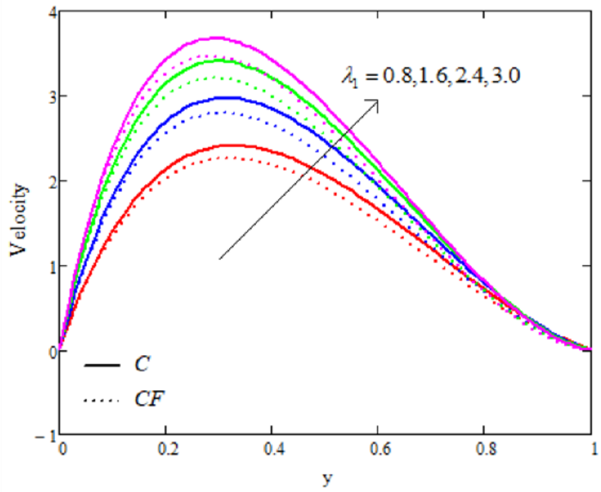

Fig. 16. Velocity plot for multiple values of λ_1 with $G_r = 5, G_c = 8$, $k = 0.2, S_c = 0.5, H_a = 0.3, \lambda = 0.9, P_r = 7, \eta = 0.3$

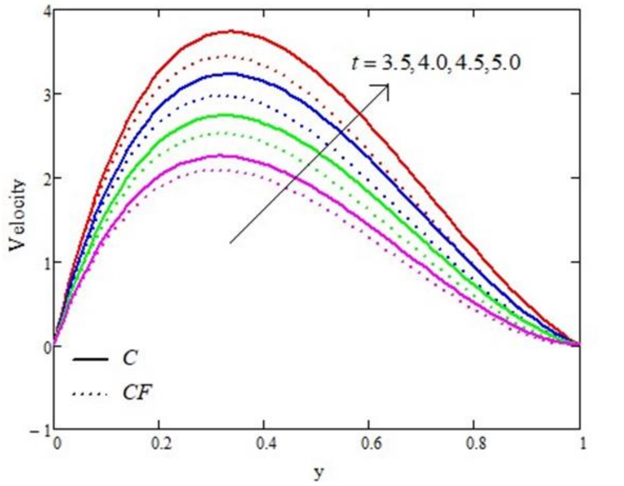

Fig. 17. Velocity plot for multiple values of t with $G_r = 5, G_c = 8, k = 0.2, S_c = 0.5, H_a = 0.3, \lambda = 0.9, \lambda_1 = 1.6, P_r = 7, \eta = 0.3$

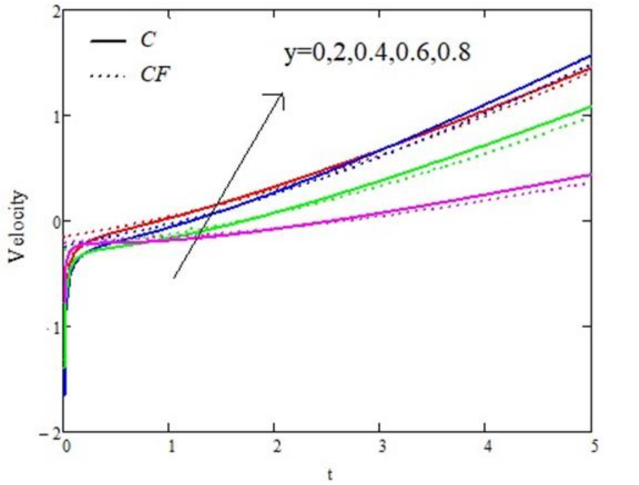

Fig. 18. Velocity plot for multiple values of y with $G_r = 5, G_c = 8, k = 0.2, S_c = 0.5, H_a = 0.3, \lambda_1 = 1.6, P_r = 7, \eta = 0.3$

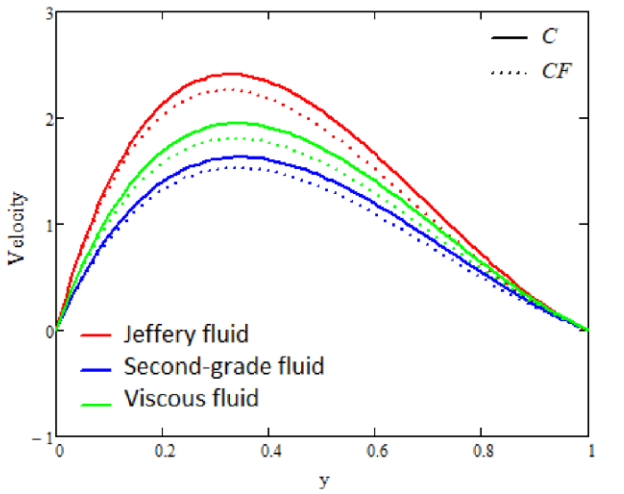

Fig. 19. Velocity plot for limiting cases

The Hartman number impacts on the velocity of the fluid, as portrayed in Fig. 14. It has been observed that an ascent in the Hartman number reduces the fluid flow. This conduct is undeniable as transverse magnetic fields resist the flow of fluid and hence result in depreciation in the velocity field.

The governing of material parameter λ on the fluid flow is elaborated in Fig. 15. It has been observed that with the enormity of λ up, a descent in the velocity curves occurs owing to an increase in the viscous forces and elasticity of the fluid.

To visualise the impact of the rheology of fluid in the presence of Jeffrey fluid parameter $\lambda1$ on the velocity curves, Fig.16 is graphed. It has been noticed that the fluid velocity boosts up as we add up the value of $\lambda1$. From the reasoning point of view, tangential stress increases, which accelerates the fluid flow.

The velocity curves for the time variation are shown in Fig. 17. The flow of the fluid accelerates as time passes.

The velocity curves versus time are shown in Fig. 18.

In the comparison between the C and CF models, we noticed that the CF model has smaller velocity, temperature and concentration curves as compared with the C model. The limiting case's velocity profile is plotted in Fig. 19.

7. FINAL REMARKS

Caputo and Caputo Fabrizio's time-fractional approach is used to analyse the Jeffrey fluid on two parallel vertical plates immersed in a permeable medium. The exact expressions for temperature, concentration and velocity are obtained using the LT. The effect of the associated implanted parameters on velocity, temperature and concentration are detailed here using graphs. The following are the final remarks:

- Increasing the fractional parameter η increases velocity, temperature and concentration.
- Temperature curves decay with the rise in P_r and time.
- Concentration profile decays with the rise in S_c and time.
- The fluid velocity slows as the values of P_r, λ, H_a, K rise.
- The enhancement in fluid flow is observed with the increase in G_r, G_c, λ_1 and S_c values.
- The C model has a higher velocity, temperature and concentration than the CF model.
- The recovered results are of integer order derivative Jeffrey fluid for $\eta \to 1$.
- The results obtained for both $\lambda \to 0$, $\lambda_1 \to 0$ and $\eta \to 1$ are for ordinary viscous fluid.

REFERENCES

1. Dunn J E, Rajagopal K R. Fluid of differential type: critical review and thermodynamic analysis, Int J Eng Sci. 1995; 33: 689-729.
2. Rajagopal K R. Mechanics of non-Newtonian fluids, in: Galdi GP, Necas J (Eds.). Recent Developments in Theoretical Fluid Mechanics in: Pitman Res Notes Math Ser Longman Scientific and Technical. New York. 1993; 291.
3. Hayat T, Sajjad R, Asghar S. Series solution for MHD channel flow of a Jeffrey fluid. Commun Nonlin Sci Numer Simulat. 2010; 15(9): 2400-6.
4. Das K, Acharya N, Kundu P K. Thermal radiation in unsteady MHD free convection flow of Jeffrey fluid. Alex. Eng. J. 2015; 54: 815.
5. Imtiaz M, Hayat T, Alsaedi A. MHD convection flow of Jeffrey fluid due to a curved stretching surface with Homogenous Reactions. PLoS ONE 2016.
6. Jena S, Mishra S R, Dash GC, Influence of non-integer order parameter and Hartmann number on the heat and mass transfer flow

DOI 10.2478/ama-2023-0068

on Jeffrey fluid over an oscillating vertical plate with Caputo-Fabrizio time fractional derivatives. Int J Appl Comp Math 2016.
7. Hussain T, Shehzad S A, Hayat T, Alsaedi A, Al-Solamy F, Ramzan M. Radiative Hydromagnetic Flow of Jeffrey Nanofluid by an Exponentially Stretching Sheet. Plos One 2014; 9: 1-9.
8. Hayat T, Mustafa M. Influence of thermal radiation on the unsteady mixed convection flow of a Jeffrey fluid over a stretching sheet.
9. Z Naturforsch. 2010; 65a: 711-719.
10. Idowu A S, Jimoh A, Ahmed LO. Impact of Heat and Mass Transfer on MHD Oscillatory Flow of Jeffrey Fluid in a Porous Channel with Thermal Conductivity. Dufour and Soret. J Appl Sci Environ Manage. 2015; 19(4): 819-830.
11. Zin N A M, Khan I, Shafie S. Influence of thermal radiation on unsteady MHD free convection flow of Jeffrey fluid over a vertical plate with ramped wall temperature. Math Probl Eng. 2016; 6257071.
12. Zeeshan A, Majeed A. Heat transfer analysis of Jeffrey fluid flow over a stretching sheet with suction/injection and magnetic dipole effect. Alexandria Eng J. 2016; 55 (3): 2171-2181.
13. Agarwal V, Singh B, Nisar K S. Numerical analysis of heat transfer in magnetohydrodynamic micropolar Jeffrey fluid flow through porous medium over a stretching sheet with thermal radiation. J Therm Anal Calorim. 2022; 147: 9829–9851.
14. Bhatti MM, Zeeshan A. Analytic study of heat transfer with variable viscosity on solid particle motion in dusty Jeffrey fluid. Mod Phys Lett B. 2016; 30 (16): 1650196.
15. Turkyilmazoglu M. Unsteady convection flow of some nanofluids past a moving vertical flat plate with heat transfer. J Heat Transfer. 2014;136 (3): 031704.
16. Bagley RL, Torvik PJ. A theoretical basis for the application of fractional calculus to viscoelasticity. J Rheol. 1983;27 (3): 201-210.
17. Jamil M, Khan NA. Slip effects on fractional viscoelastic fluids. Intern. J Different Equat 2011.
18. El Kot MA, Abd Elmaboud Y. Unsteady pulsatile fractional Maxwell viscoelastic blood flow with Cattaneo heat flux through a vertical stenosed artery with body acceleration. J Therm Anal Calorim. 2022;147:4355-4368.
19. Riaz MB, Siddiqui I, Saeed ST, Atangana A. MHD Oldroyd-B Fluid with Slip Condition in view of Local and Nonlocal Kernels. J Appl Comput Mech. 2021;7(1): 116-127.
20. Alsharif M, Abdellateef AI, Abd Elmaboud Y. Electroosmotic flow of fractional Oldroyd-B fluid through a vertical microchannel filled with a homogeneous porous medium: Numerical and semianalytical solutions. Heat Transfer. 2022; 51(5): 4033-4052.
21. Khan I, Shah NA, Vieru D. Unsteady flow of generalized Casson fluid with fractional derivative due to an infinite plate. Eur Phys J Plus. 2016; 131 (6): 1-12.
22. Imran MA, Shah NA, Aleem M et al. Heat transfer analysis of fractional second-grade fluid subject to Newtonian heating with Caputo and Caputo-Fabrizio fractional derivatives: A comparison. Eur Phys J Plus. 2017; 132: 340-358.
23. Abdellateef I, Alshehri HM, Abd Elmaboud Y. Electro-osmotic flow of fractional second-grade fluid with fractional Cattaneo heat flux through a vertical microchannel. Heat Transfer. 2021; 50(7): 6628-6644.
24. Alsharif AM, Abd Elmaboud Y. Electroosmotic flow of generalized fractional second grade fluid with fractional Cattaneo model through a vertical annulus. Chinese Journal of Physics. 2022; 77: 1015-1028.
25. Saqib M, Ali F, Khan I, Sheikh NA, Jan SAA. Exact solutions for free convection flow of generalized Jeffrey fluid: a Caputo-Fabrizio fractional model. Alexandria Engineering Journal. 2018; 57(3): 18491858.
26. Shehzad SA, Hayat T, Alhuthali MS, Asghar S. MHD three-dimensional flow of Jeffrey fluid with Newtonian heating. J Cent South Univ. 2014; 21: 1428-1433.
27. Hayat T, Sajjad R, Asghar S. Series solution for MHD channel flow of a Jeffrey fluid. Commun Nonlin Sci Numer Simulat. 2010; 15(9): 2400-6.
28. Farman M, Besbes H, Nisar KS, Omri M. Analysis and dynamical transmission of Covid-19 model by using Caputo-Fabrizio derivative. Alexandria Engineering Journal. 2023; 66: 597-606.
29. Liu Y, Zheng L, Zhang X. Unsteady MHD Couette flow of a generalized Oldroyd-B fluid with fractional derivative. Comput Math Appl. 2011; 61: 443-450.
30. Hilfer R. Applications of Fractional Calculus in Physics. World Scientific Press. Singapore 2000.
31. Tan W, Pan W, Xu M. A note on unsteady flows of a viscoelastic fluid with the fractional Maxwell model between two parallel plates. Internat J Non-Linear Mech. 2003;38: 645-650.
32. Wang S, Xu M. Exact solution on unsteady Couette flow of generalized Maxwell fluid with fractional derivatives. Acta Mech. 2006;187: 1-4.
33. Qi HT, Jin H. Unsteady rotating flows of viscoelastic fluid with the fractional Maxwell model between coaxial cylinders. Acta Mech Sin. 2006; 22: 301-305.
34. Siddique I, Sajid Z. Exact solutions for the unsteady axial flow of non-Newtonian fluids through a circular cylinder. Commun Nonlinear Sci Numer Simul. 2011; 16: 226-238.
35. Vieru D, Fetecau C, Fetecau C. Time-fractional free convection flow near a vertical plate with Newtonian heating and mass diffusion. Therm Sci. 2015; 19 (1): S85–S98.
36. Iftikhar N, Baleanu D, Riaz MB, Husnine SM. Heat and Mass Transfer of Natural Convective Flow with Slanted Magnetic Field via Fractional Operators. J Appl Comput Mech. 2021; 7(1): 189-212.
37. Iftikhar N, Saeed ST, Riaz MB. Fractional study on heat and mass transfer of MHD Oldroyd-B fluid with ramped velocity and temperature. Computational Methods for Differential Equations 2021. 2021: 1-28.
38. Dharmendar Reddy Y, Shankar Goud B, Nisar KS, Alshahrani B, Mahmoud M, Park C. Heat absorption/generation effect on MHD heat transfer fluid flow along a stretching cylinder with a porous medium. Alexandria Engineering Journal. 2023; 64: 659-666.
39. Zafar A, Awrejcewicz J, Mazur O, Riaz MB. Study of composite fractional relaxation differential equation using fractional operators with and without singular kernels and special functions. Advances in Difference Equations 2021. 2021: 87.
40. Aleem M, Asjad MI, Ahmadian A, Massimiano Ferrara MS. Heat transfer analysis of channel flow of MHD Jeffrey fluid subject to generalized boundary conditions. Eur Phys J Plus. 2020; 135:26.
41. Asgir M, Abualnaja KM, Zafar AA, Riaz MB, Abbas M. Special function form exact solutions for Jeffrey fluid: An application of power law kernel (submitted).
42. Butt AR, Abdullah M, Raza N, Imran MA. Influence of non-integer order parameter and Hartmann number on the heat and mass transfer flow of a Jeffrey fluid over an oscillating vertical plate via Caputo Fabrizio. Euro Phys J Plus. 2017; 132(10): 4-14.
43. Imran MA, Aleem M, Chowdhury MSR, Hussnain A. Analysis of mathematical model of fractional viscous fluid through a vertical rectangular channel. Chin J Phys. 2019; 61: 336-50.

Maryam Asgir: https://orcid.org/0009-0006-0654-4836

Muhammad Bilal Riaz: https://orcid.org/0000-0001-5153-297X

Ayesha Islam: https://orcid.org/0000-0003-0372-5261